SINAPSE

13th Annual Scientific Meeting 2021

Programme and Abstracts Booklet

1495 University of Aberdeen

University of Dundee

The University of Edinburgh

University of Glasgow

University of St Andrews

University of Stirling

University of Strathclyde

Chief Scientist Office

Supported by:

Thursday 16th September 2021			
Hopin			
1020	**Gather**		
Plenary Session 1 **Chair: Dr Jennifer Macfarlane**			
1030	**Welcome – Dr William McGeown, University of Strathclyde**		
1035	**Welcome – Dr Jennifer Macfarlane, SINAPSE Director, NHS Tayside**		
1040	**Keynote: *Connectome based spreading of pathology and factors of resilience in Alzheimer's disease* - Prof Michael Ewers, Institute for Stroke and Dementia Research, University of Munich**		
1140	**Poster Lightning Pitches 1-12**		
1200	**Lunch (60 mins)**		
Parallel Sessions – See Next Page for Details on Talks			
1300	**Session 1 – Neuroimaging**	**Session 2 – Breast Cancer**	**Session 3 – Ultrasound & Misc**
1400	**Tea Break (30 mins)**		
Plenary Session 2 **Chair: Dr Richard Mosses**			
1430	**Keynote: *The development of Imaging Biomarkers is a multi-disciplinary process* - Dr Anna Barnes, King's College London**		
1530	**Keynote: *Imaging in robotic endoscopy, from autonomous navigation to diagnosis* - Dr Bruno Scaglioni, University of Leeds**		
1615	**Short Break (10mins)**		
1625	**Virtual Social Event** *An opportunity to meet new colleagues and/or catch up with those you haven't seen in a while*		
1730	**Close**		

Parallel Sessions (1300-1400)

Session 1 – Neuroimaging **Chair: Dr Magdalena Ietswaart, University of Stirling**			
1300	*Dynamic functional networks in Alzheimer's disease, mild-cognitive impairment, and healthy ageing*	Nicolas Rubido, University of Aberdeen	O01
1315	*Delusions in Alzheimer's disease: neuroanatomical, cognitive and psychiatric correlates*	Sara Scarfo, University of Strathclyde	O02
1330	*The Impact of Brain Iron on Neurodegeneration and Cognitive Decline*	Holly Spence, University of Aberdeen	O03
1345	*From cognition to molecules: tracking Alzheimer's disease with cognitive biomarkers*	Mario Parra, University of Strathclyde	O04

Session 2 – Breast Cancer **Chair: Dr Sarah Savaridas, NHS Tayside**			
1300	*Lipid composition in peri-tumoural adipose tissue in postmenopausal patients with breast cancer*	Sai Man Cheung, University of Aberdeen	O05
1315	*Peri-tumoural spatial distribution of lipid composition and tumour cellular differentiation in breast cancer*	Sai Man Cheung, University of Aberdeen	O06
1330	*Are baseline mammographic and ultrasound features associated with metastasis free survival in women receiving neoadjuvant chemotherapy for invasive breast cancer?*	Andy Evans, University of Dundee	O07
1345	*Is skin thickening and enhancement on breast MRI associated with metastasis-free survival (MFS)?*	Valentine Mberu, University of Dundee	O08

Session 3 – Ultrasound and Miscellaneous Topics **Chair: Dr Rosalind Mitchell-Hay, NHS Grampian**			
1300	*Scotland's First MR Guided Focused Ultrasound Surgical Treatment*	Dr Jennifer Macfarlane, NHS Tayside	O09
1315	*Segmentation of Thalamic Nuclei for Targeting MR Guided Focused Ultrasound Surgery*	Graeme Mackenzie, Ninewells Hospital	O10
1330	*Examining Cognitive Aspects of Relevance Judgement*	Zuzana Pinkosova, University of Strathclyde	O11

Friday 17th September 2021			
Hopin			
0945	**Gather**		
Plenary Session 3			
0955	***Developing advanced imaging as a tool for precision medicine in The Living Laboratory* – Dr Kristin Flegal, University of Glasgow O12**		
1015	**ECR Rising Star: *Magnetic resonance elastography of the brain and its application in dementia research* - Dr Lucy Hiscox, University of Bath**		
1100	**Poster Lightning Pitches 13-25**		
1130	**Tea break (30 mins)**		
Parallel Sessions – See Next Page for Details on Talks			
1200	**Session 4 – Neuroimaging Methods**	**Session 5 – Preclinical & Optical Imaging**	**Session 6 - Vascular**
1315	**Lunch (45 mins)**		
Plenary Session 4			
1400	**Keynote: *CCTA for planning coronary intervention - lessons from TAVR* - Dr Jonathan Leipsic, University of British Columbia**		
1500	**Closing Remarks and Prize Giving – Dr Jennifer Macfarlane, NHS Tayside**		
1510	**Main Programme Close**		
Workshops			
1500	**SCCT**		
1530	**NVIDIA**		

Parallel Sessions (1200-1315)

Session 4 – Neuroimaging Methods **Chair: Prof Adam Waldman, University of Edinburgh**			
1200	*Automated brain tumour identification using magnetic resonance imaging: a systematic review and meta-analysis*	Omar Kouli, University of Dundee	O13
1215	*Joint multi-field T1 quantification for Fast Field-Cycling imaging identifies ischaemic stroke at magnetic field strength below 20 mT*	Vasiliki Mallikourti, University of Aberdeen	O14
1230	*Eigenvector alignment: Assessing functional network changes in Alzheimer's disease*	Ruaridh Clark, University of Glasgow	O15
1245	*Efficiency of marking and rendering software for epilepsy surgery*	Mateo Gregory, University of Edinburgh	O16
1300	*Measurement of microbubble backscattering signals in 3D-printed, physiologically-relevant platforms*	Dr Roger Domingo-Roca, University of Strathclyde	O17

Session 5 – Preclinical and Optical Imaging **Chair: Dr Gordon Waiter, University of Aberdeen**			
1200	*Direct imaging of glymphatic transport using H217O MRI*	Alaa Alghanimy, University of Glasgow	O18
1215	*Comparison of [18F]MNI-1038 (racemate) and [18F]MNI-1126 (R-enantiomer) kinetics in the mouse brain*	Catriona Wimberley, University of Edinburgh	O19
1230	*Mesoscopic imaging of pediatric palatine tonsil infection*	Megan Clapperton, University of Strathclyde	O20
1245	*Towards Robust Real-World Decision Support for Skin Lesion Diagnosis*	Jacob Carse, University of Dundee	O21

Session 6 – Vascular **Chair: Dr Michelle Williams, University of Edinburgh**			
1200	*Strain estimation in aortic roots from 4D echocardiographic images using medial modelling and deformable registration*	Peter Mortensen, University of Glasgow	O22
1215	*Quantitative Comparison of Arterial Spin Labelling Imaging Sequence in Ischaemic Stroke Patients: A Bland-Altman Analysis*	Zanariah Mohd, University of Glasgow	O23
1230	*68Ga-FAPI as a marker of fibrosis activity and matrix remodelling in patients with myocardial infarction*	Anna Barton, University of Edinburgh	O24
1245	*Synthetic workflow for validation of wall shear stress estimated using plane wave in carotid stenosis*	Ke Yang, University of Dundee	O25
1300	*Longitudinal TSPO PET imaging with [18F]LW223 in a rat myocardial infarction model*	Mark MacAskill, University of Edinburgh	O26

Poster Session

Poster Number	Title	Presenting Author
P1	*Potential solution to stop the improper use of abdominal x-rays for abdominal pain*	Winnie Tam
P2	*Analysis of Positron Emission Tomography Data for Tumour Detection and Delineation*	Wenhui Zhang
P3	*Sex differences in the murine brain identified using [18F]LW223 PET, a marker of TSPO expression in vivo*	Agne Knyzeliene
P4	*Brain Networks: Challenges of high correlations and how to overcome them.*	Philipp Loske
P5	*Pre-operative Coronary Artery Calcification (CAC) in patients undergoing potentially curative colorectal cancer surgery*	Shea Roddy
P6	*Are Reported Volume Abnormalities in Autism Consistent? A Meta-Analysis of Morphometric Data*	Michelle Sader
P7	*A Meta-Analytic Investigation of Grey Matter changes in Anorexia Nervosa*	Michelle Sader
P8	*The Cerebellum Plays More Than One Role in Appetite Control: Evidence from Typical and Pathological Populations*	Michelle Sader
P9	*Comparing Specific Absorption Rate (Tissue Heating) Management Methods for Parallel Transmit MRI at 7 Tesla*	Sydney Williams
P10	*Drug discovery and repurposing using biomimetic chromatography and body-on-chip technology.*	Liam Carr
P11	*Machine Learning methods for the classification of Dementia using images from the Genetics of Diabetes Audit and Research in Tayside Scotland (GoDARTS) cohort*	Esma Mansouri-Benssassi
P12	Withdrawn	
P13	*Providing a neuro-imaging evidence-base for motor neuro-rehabilitation*	Magda Mustile
P14	*3D-printed tissue-mimicking and cell compatible hybrid hydrogels for ultrasound and microbubble-mediated drug delivery research*	Lauren Gilmour
P15	*Low Cost Photoacoustic Computed Tomography System Based on Adaptive Back Projection Reconstruction*	Yang Zhang
P16	*Assessment of Lungman Anthropomorphic Phantom*	Amy Oana
P17	*Developing new biomarkers for imaging oligodendrocyte function in vivo.*	Robert Shaw
P18	*Study to establish the parameter space of ultrasound imaging based detection of tissue stiffness variations*	Patricia Foia
P19	*Association of the regional cortical complexity with fluid cognition and life course factors*	Nafeesa Nazlee
P20	*Evaluation of the stiffness of flexor digitorum superficialis muscle using ultrasound shear wave elastography in healthy volunteer: a preliminary study*	Phongpan Tantipoon
P21	*Improving Needle Visualization in Ultrasound-Guided Regional Anaesthesia*	Ashraf Agweder
P22	*Application of Swept-Source Optical Coherence Tomography (SS-OCT) System for Wound Healing Monitoring based on a Murine Model*	Tianyu Zhang

P23	*Using deep learning and transfer learning to accurately assess the epithelial region in human skin based on Optical Coherence Tomography*	Yubo Ji
P24	*Viscoelastic properties of a corneal stromal model measured by surface acoustic wave optical coherence elastography (SAW-OCE)*	Yilong Zhang
P25	*Assessment of MR imaging quality with MRgFUS installation*	Katherine McLellan
P26	*Is diagnostic imaging of the breast possible with a Magseed in situ?*	Jennifer Summersgill
P27	*Optimising Navigator Scans for Use in MRI Prospective Motion Correction*	Steven Winata
P28	Withdrawn	
P29	*RF simulations of cranial fixation plates in 7 tesla MRI*	Andrew McDevitt
P30	*Ex-vivo investigation of inflammation and thrombus PET radiotracers in lung, heart and brain tissue from COVID-19 related deaths*	Mark MacAskill
P31	*Characterisation of a Diffusion Phantom used for Diffusion MRI QA*	Christopher Taylor
P32	*Lymph node characterisation of a metastatic mouse model of CRC using pre-clinical ultrasound*	Marion Bacou
P33	Withdrawn	
P34	*SAR Simulation of a Close-fitting 8-channel Transceiver Head Coil Including EEG Electrodes for Safety Validation at 7T*	Paul McElhinney
P35	*Contrast enhanced magneto-motive ultrasound (CE- MMUS) as a promising imaging technique for improved lymph node identification*	Katarzyna Kaczmarek

Abstracts

Keynote Talks

Keynote 1

Connectome based spreading of pathology and factors of resilience in Alzheimer's disease

Professor Michael Ewers

Institute for Stroke and Dementia Research, Ludwig Maximilian University Munich

Abstract: Tau pathology is the major driver of clinical progression in Alzheimer's disease, however, those factors that shape the spreading of tau pathology in the brain and modulate its effect on cognition are unclear. In the current talk, I will first discuss genetic variants that increase the likelihood to develop tau pathology. Specifically, we recently identified the major AD risk variant BIN1 to enhance fibrillar tau (Franzmeier et al. Nature Commun, 2019), whereas the lifespan-prolonging Klotho VS SNP protects against tau pathology (Neitzel et al. Nature Commun, 2021), pointing to specific mechanisms of higher susceptibility vs resistance against tau pathology. Whereas these genetic variants influence the development of tau globally in the brain, it is the functional architecture of the brain that shapes the spatial pattern of the spreading of tau pathology during the course of AD. In a series of studies using tau PET combined with functional connectomics, we found that the spreading of tau pathology from epicenters of initial high tau burden occurs preferentially to closely connected brain regions, suggesting that the functional connectome routes the progression of tau pathology between brain regions (Franzmeier et al. Nature Comm 2019, Sci Advances 2020). Finally, I will discuss factors that underlie cognitive resilience against the effects of tau pathology. We have identified key topological features of the functional connectome such as enhanced hub connectivity of the cognitive control network and higher global network segregation (Ewers et al. Brain 2021) to support cognitive resilience in both late-onset AD and autosomal dominant AD. In summary, I will discuss putative factors the influence the development of tau pathology as well downstream effects of tau on cognitive symptoms in AD.

Biography: Dr Michael Ewers received his PhD in Cognitive Psychology in 2003, following a Fulbright scholarship in 1998. Michael worked as a post-doc at the Ludwig Maximilian University, and subsequently as research scientist at institutions including Trinity College Dublin (Ireland) and University of California at San Francisco (USA). Since 2012 he is Associate Professor at the Ludwig-Maximilian-University Munich. Michael Ewers is head of the neuroimaging facility at the Institute of Stroke and Dementia Research at the University Hospital, LMU and is leading a research group on neuroimaging and biomarker research in Alzheimer's disease.

Michael Ewers' lab combines functional connectomics, genetics and molecular PET markers to model the spatiotemporal evolution of fibrillar tau and beta-amyloid. The lab has developed connectome-based prediction models for the patient-tailored prediction of tau pathology. Another major research centers on the understanding of reserve and resilience in Alzheimer's disease. Through a series of functional MRI studies, his lab showed that graph theoretical network analysis is useful to understand major hubs that support cognitive resilience in Alzheimer's disease (Franzmeier et al. Brain, 2018, Ewers et al. Brain 2020). Furthermore he demonstrated in collaboration with Dr Christian Haass that higher levels of soluble TREM2, a biomarker of microglia activity, is associated with higher resilience against the development of Alzheimer pathology (Ewers et al. Science Translational Medicine, 2019; Ewers et al. EMBO Mol Med 2020). He was co-founder of the PIA on Reserve, Resilience and Protective factors of the ISTAART. Michael Ewers is senior editor of the Alzheimer Association's journal Alzheimer's & Dementia, and has published over 130 publications with > 10000 citations, and an H-index of 56 (Google scholar). Dr. Ewers

received several awards, most recently the deLeon Senior Researcher Prize 2021 at the Alzheimer's Association International Conference (AAIC).

Keynote 2

The development of Imaging Biomarkers is a multi-disciplinary process

Dr Anna Barnes

King's College London

Abstract: Imaging biomarkers: biologically relevant, disease sensitive and robust

Several years ago, the Cancer Research UK charity recognised the importance of imaging biomarkers in understanding the mechanisms of cancer, developing treatments and monitoring the response to existing and new treatments. Alongside their multi-disciplinary programme grant they launched an imaging biomarker roadmap.

My talk will explore this framework and the role of the medical physicist and clinical engineer in embedding the pathway into current research practices. This exploration will finish with an introduction to a systems approach to health and care design and continuous improvement (Clarkson et al 2018).

Biography: Dr Anna Barnes has a PhD in neuroimaging from the University of Glasgow and became a registered clinical scientist in 1997. She has held post-doctoral fellowships at the university of New York, Columbia University NYC, University of Cambridge and University College London. She is currently Director of the King's College Technical Evaluation Centre and Honorary Consultant Clinical Scientist at Guy's and St Thomas' Hospital London.

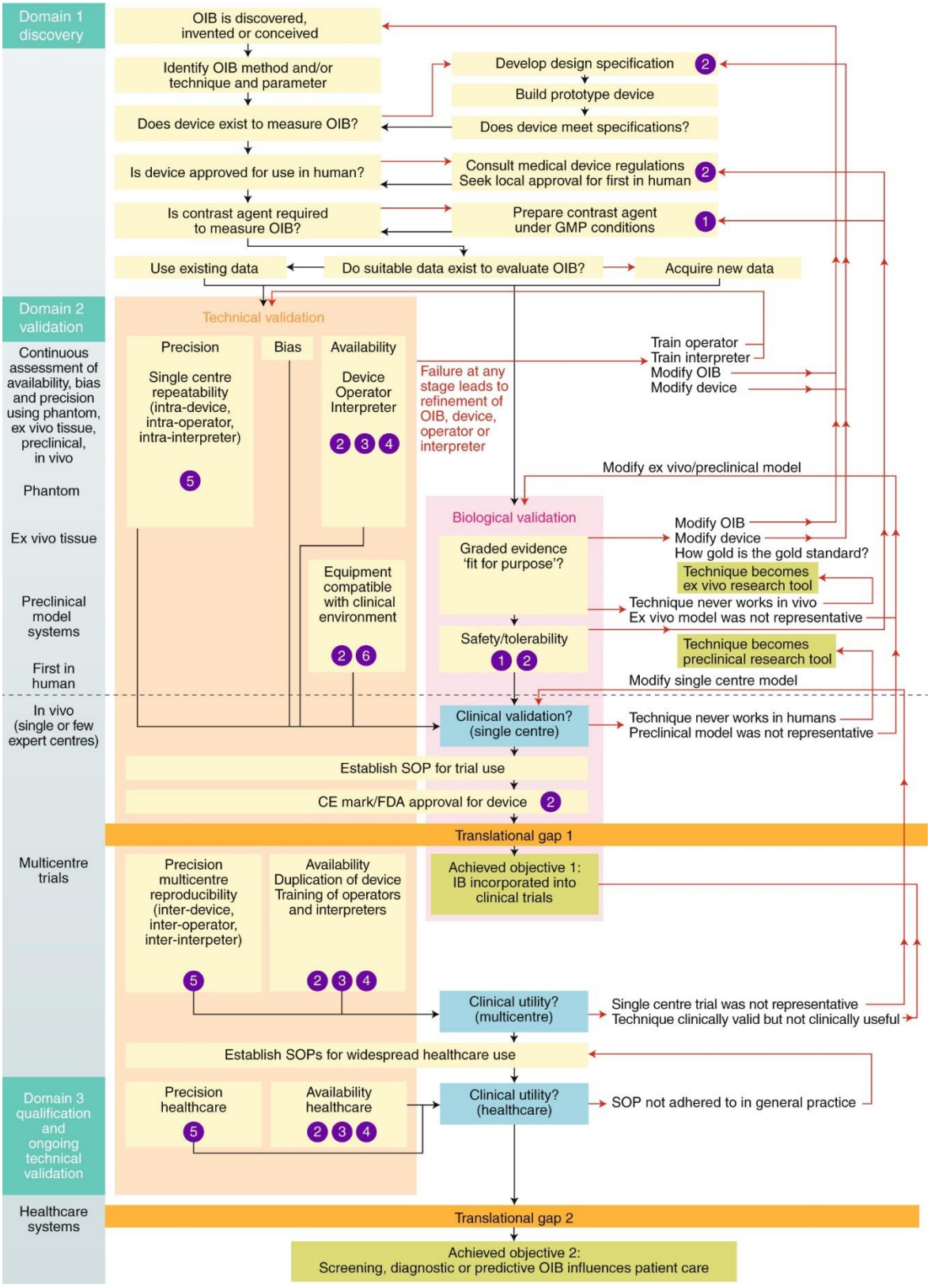
Domain 1 discovery
OIB is discovered, invented or conceived
Identify OIB method and/or technique and parameter
Does device exist to measure OIB?
Develop design specification 2
Build prototype device
Does device meet specifications?
Is device approved for use in human?
Consult medical device regulations
Seek local approval for first in human 2
Is contrast agent required to measure OIB?
Prepare contrast agent under GMP conditions 1
Use existing data
Do suitable data exist to evaluate OIB?
Acquire new data
Domain 2 validation
Technical validation
Precision
Bias
Availability
Single centre repeatability (intra-device, intra-operator, intra-interpreter) 5
Device Operator Interpreter 2 3 4
Failure at any stage leads to refinement of OIB, device, operator or interpreter
Train operator
Train interpreter
Modify OIB
Modify device
Modify ex vivo/preclinical model
Biological validation
Graded evidence 'fit for purpose'?
Modify OIB
Modify device
How gold is the gold standard?
Technique becomes ex vivo research tool
Technique never works in vivo
Ex vivo model was not representative
Safety/tolerability 1 2
Technique becomes preclinical research tool
Equipment compatible with clinical environment 2 6
Modify single centre model
Clinical validation? (single centre)
Technique never works in humans
Preclinical model was not representative
Establish SOP for trial use
CE mark/FDA approval for device 2
Translational gap 1
Achieved objective 1: IB incorporated into clinical trials
Precision multicentre reproducibility (inter-device, inter-operator, inter-interpeter) 5
Availability Duplication of device Training of operators and interpreters 2 3 4
Clinical utility? (multicentre)
Single centre trial was not representative
Technique clinically valid but not clinically useful
Establish SOPs for widespread healthcare use
Domain 3 qualification and ongoing technical validation
Precision healthcare 5
Availability healthcare 2 3 4
Clinical utility? (healthcare)
SOP not adhered to in general practice
Healthcare systems
Translational gap 2
Achieved objective 2: Screening, diagnostic or predictive OIB influences patient care
Continuous assessment of availability, bias and precision using phantom, ex vivo tissue, preclinical, in vivo
Phantom
Ex vivo tissue
Preclinical model systems
First in human
In vivo (single or few expert centres)
Multicentre trials

Keynote 3

Imaging in robotic endoscopy, from autonomous navigation to diagnosis

Dr Bruno Scaglioni

University of Leeds

Abstract: Endoscopy is among the most complex clinical activities, often requiring long training of the endoscopist manual ability to navigate the body. Robotic endoscopy can solve all the major drawbacks of traditional endoscopes, simultaneously posing a new opportunity: autonomy. Tasks like navigation, biopsy and lesions' treatment can be performed autonomously with robotics. In this context, advanced imaging plays a paramount role in guiding the robot through unstructured environments. In this talk, the most eminent challenges of image-based autonomous endoscopy will be discussed, ranging from navigation to diagnosis and treatment.

Biography: Bruno Scaglioni received his Ph.D. in Systems and Controls at the Politecnico di Milano in 2017. Since then, his research interests focused on surgical robotics, autonomous execution of surgical tasks and autonomous endoscopy. He is currently Research Fellow in medical robotics at the university of Leeds where he leads the research on several projects, all centred around the idea of reducing the manual dexterity required to surgeons by enhancing the autonomy of medical devices.

ECR Rising Star

Magnetic resonance elastography of the brain and its application in dementia research

Dr Lucy Hiscox

University of Bath

Abstract: The increasing prevalence of Alzheimer's disease and other dementias has provided motivation for developing new imaging methods for understanding more about the etiology of such diseases as well as the effectiveness of potential treatments. Magnetic resonance elastography (MRE) is a phase-contrast MRI-based method for quantitatively imaging the shear tissue stiffness (mechanical properties) in vivo and is now routinely used clinically as a non-invasive tool to assess the severity of hepatic diseases. Due to significant technical and engineering innovations to MRE hardware equipment, imaging pulse sequences, and inversion algorithms for calculating tissue mechanical properties, brain MRE has become a sensitive, high-resolution, and reliable neuroimaging technique. As tissue stiffness acts a proxy for the health and integrity of the underlying microstructure, an increasing number of research groups have begun to investigate whether MRE can help in the assessment and diagnosis of a range of neurological and neurodegenerative diseases. In this talk, I provide an overview of how technical innovations in brain MRE have increasingly improved our understanding of conditions such as Alzheimer's disease, Parkinson's disease, and frontotemporal dementia, and how complementary ex vivo studies have begun to shed light on the biological mechanisms that give rise to changes in mechanical property measurements. I will also discuss more recent work that has uncovered significant viscoelastic structure-function relationships, particularly involving the hippocampus and memory, and which ultimately suggests that brain MRE could become a valuable non-invasive imaging biomarker for the early detection of pre-clinical dementia.

Biography: Lucy Hiscox is a Postdoctoral Research Fellow at the University of Bath. She graduated with a BSc in Psychology from Cardiff University before obtaining her PhD in Neuroscience funded by Alzheimer Scotland at the University of Edinburgh in 2018. Lucy then spent two years within the Department of Biomedical Engineering at the University of Delaware managing a NIH-funded clinical trial on brain mechanical properties, measured with magnetic resonance elastography (MRE), and their relationship with aging, cognition, and disease. Lucy was elected as a Trainee Representative for the MRE study group at the International Society for Magnetic Resonance in Medicine (ISMRM) in 2019 and was recipient of the Magna Cum Laude Award for work related to MRE and Alzheimer's Disease.

Keynote 4

CCTA for planning coronary intervention - lessons from TAVR

Dr Jonathan Leipsic

University of British Columbia

Abstract: Coronary CTA has established itself as the first line diagnostic test for the evaluation of symptomatic patients with suspected but not confirmed coronary artery disease. It offers excellent diagnostic accuracy, incremental prognostic information, and allows for the titration of medical therapy in a fashion that improves clinical outcomes.

With CCTA being used more frequently there is the opportunity to use it to help guide coronary intervention. By providing fluoroscopic angles, lesion length and morphology, physiology (ffrct) and perhaps even allowing the modeling of the physiological improvement following pci the opportunities to help guide pci are real and will be discussed in this lecture.

Biography: Dr Leipsic is the Chairman of the Department of Radiology for Providence Health Care, Vancouver Coastal Health and the Vice Chairman of Research for the UBC Department of Radiology. He is a Professor of Radiology and Cardiology with the University of British Columbia. Dr Leipsic is also a Canada Research Chair in Advanced Cardiopulmonary Imaging. Dr Leipsic has over 530 peer reviewed manuscripts in press or in print, over 300 scientific abstracts, and editor of 2 textbooks. He speaks internationally on a number of cardiopulmonary imaging topics with over 150 invited lectures in the last 4 years. He is also past President of the Society of Cardiovascular CT (2015-2016) and was awarded its Gold Medal in 2019 and was recently named to the prestigious Top 1% most impactful scientist designation by the Web of Science in 2019.

Parallel Sessions

Abstract number: O01

Dynamic functional networks in Alzheimer's disease, mild-cognitive impairment, and healthy ageing

Nicolás Rubido[1,2] and Vesna Vuksanović[3,4]

1. University of Aberdeen, Aberdeen Biomedical Imaging Centre, Ab25 2ZG Aberdeen, United Kingdom

2. Universidad de la República, Instituto de Física de Facultad de Ciencias, 11400 Montevideo, Uruguay

3. Swansea University Medical School, Swansea University, SA2 8PP Swansea, United Kingdom

4. Health-Data Research United Kingdom, Swansea University

The analysis of brain networks from functional MRI (fMRI) has helped to better understand the cortical activity and its changes in neurodegenerative disorders that cause dementia. Here, we present a comparative analysis of dynamic functional brain networks in individuals with Alzheimer's disease (AD), Mild Cognitive Impairment (MCI) and cognitively normal healthy elderly (HE). We have analysed consistency and differences of the functional networks between the study groups at the lobe level using two well established brain parcellations (brain atlases). Our results show common and distinct patterns of dynamic brain connectivity between the groups.

Acknowledgements: This work was supported by the Roland Sutton Academic Trust (research grant no. RG13688)

Contact: nicolas.rubidoobrer@abdn.ac.uk

Abstract number: O02

Delusions in Alzheimer's disease: neuroanatomical, cognitive and psychiatric correlates

Sara Scarfo[1], William McGeown[1]

1. Psychological Sciences and Health, University of Strathclyde

Experienced by approximately half of people with Alzheimer's Disease (AD) and Mild Cognitive Impairment (MCI), delusions are among the most prevalent neuropsychiatric symptoms; they are associated with increased distress for the individuals and their caregivers, poorer disease outcome brought about by a more rapid cognitive decline, worst real-life functioning, and increased mortality. The severity of adverse outcomes and high prevalence make delusions an important research target, as clarifying their underlying mechanisms has potential to improve earlier detection and inform treatment strategies. Therefore, the current study assessed the vulnerability factors previously identified in the literature, investigating the role of neuroanatomical, cognitive, psychiatric, psychosocial, and demographic features in the manifestation of delusions. A correlational study was designed, and a sample of 91 (59 MCI and 32 AD) patients with delusions, and 91 controls (59 MCI and 32 AD patients without delusions) was selected using the Alzheimer's Disease Neuroimaging Initiative database. Delusions were measured using the Neuropsychiatric Inventory; the neuroanatomical correlates were investigated using MRI images analysed with the FreeSurfer software; the Alzheimer's Disease Assessment Scale, the Clock Drawing Test, the Trail Making Test, the Everyday Cognition and the Montreal Cognitive Assessment Test assessed cognitive function; the Neuropsychiatric Inventory and Geriatric Depression Scale measured depression. Regression models were performed, which highlighted associations between: the left anterior cingulate cortex and presence of delusions at the same timepoint; the left parahippocampal, right pars opercularis and right entorhinal cortex and later manifestation of delusions; executive and visuospatial functions, and attention and the presence and severity of delusions at the same timepoint; executive and visuospatial functions, memory and attention and later manifestation of delusions; lastly, the presence and severity of depression with later manifestation of delusions. These results suggest that specific neuroanatomical, cognitive, and psychiatric features may be involved in the delusional development.

Contact: sara.scarfo.2020@uni.strath.ac.uk

Abstract number: O03

The Impact of Brain Iron on Neurodegeneration and Cognitive Decline

Holly Spence[1], Dr Gordon Waiter[1], Dr Chris McNeil[1]

1. Aberdeen Biomedical Imaging Centre, University of Aberdeen

Iron accumulation in the brain, as measured by magnetic resonance imaging (MRI), is observed in many neurodegenerative diseases including Parkinson's disease, Alzheimer's disease, Amyotrophic Lateral Sclerosis and more. In our systematic review, we have shown that brain iron deposition, particularly in the striatal and deep grey matter regions, is associated with cognitive decline in both neurodegenerative disease and in healthy individuals. We also showed that iron accumulation in specific brain regions was associated with detrimental effects on function specific to those regions. Although these associations are known, it remains unclear whether brain iron is a cause or consequence of mechanisms of neurodegeneration and age-related cognitive decline.

The current work explores the relationships between brain iron and cognitive ability in participants of the STRADL (Stratifying Resilience and Depression Longitudinally) and ACONF (Aberdeen Children of the 1950's) cohorts of the Generation Scotland project. Susceptibility weighted MRI scans already obtained from these participants have been used to quantify regional brain iron levels, by applying a novel image analysis technique, Quantitative Susceptibility Mapping (QSM). These participants have also undergone several cognitive ability assessments, including logical memory tests, digit symbol coding, verbal fluency test, mill hill vocabulary test and matrix reasoning test. We will then measure circulating iron status, inflammatory markers and glutathione peroxidase activity (involved in iron-mediated cell death). We aim to explore associations between brain iron level and cognitive ability in this cohort, which along-side circulating measures of iron and inflammatory homeostasis could help elucidate mechanisms underlying brain iron accumulation, neurodegeneration and age-related cognitive decline.

Contact: h.spence.19@abdn.ac.uk

Abstract number: O04

From cognition to molecules: tracking Alzheimer's disease with cognitive biomarkers

Mario A Parra

School of Psychological Sciences and Health, University of Strathclyde

With the advent of promising treatments to prevent dementia caused by Alzheimer's disease (AD), we need affordable methodologies to screen for risk as early as possible. We have recently investigated the ability of a novel memory maker for AD, namely the Short-Term Memory Binding (STMB) Test, to inform about underlying pathology. In this presentation I will share the results from recent studies that revealed associations between STMB impairments and the accumulation of amyloid (Aβ) in the brain of people holding different risk levels for AD prior to overt tau pathology and neurodegeneration. The STMB Test is a simple assessment tool that can help identify people who would potentially benefit from prevention treatments.

Contact: mario.parra-rodriguez@strath.ac.uk

Abstract number: O05

Lipid composition in peri-tumoural adipose tissue in postmenopausal patients with breast cancer

Sai Man Cheung[1], Vasiliki Mallikourti[1], Tanja Gagliardi[1], Ehab Husain[2], Yazan Masannat[3], Steven D Heys[1], Jiabao He[1]

1. Institute of Medical Sciences, University of Aberdeen
2. Pathology Department, Aberdeen Royal Infirmary
3. Breast Unit, Aberdeen Royal Infirmary

Background: Targeted surveillance and early detection are critical for combating high prevalence of breast cancer in postmenopausal women, with tumour initiating hormones primarily generated in mammary adipocytes. Peri-tumoural lipid composition, proposed as the precursor of disease onset, showed diverse experimental evidence owing to limitations in methodology and study design. We set out to examine the peri-tumoural lipid composition in postmenopausal women with breast cancer.

Methods: Fourteen patients (age 53 – 71 years) with invasive ductal carcinoma and 15 age-matched controls were recruited. Double-quantum filtered correlation spectroscopy spectra were acquired on a 3 T whole body clinical MRI scanner (Achieva TX, Philips Healthcare) from peri-tumoural adipose tissue and contralateral breast in patients, and healthy breasts in controls. The spectral peaks of unsaturated bond index (UBI), triglycerides (TRG), monounsaturated fatty acids (MUFA), polyunsaturated fatty acids (PUFA) were quantified for each breast, and disparity computed as the normalised difference between breasts.

Results: There were no significant differences in UBI, TRG, MUFA and PUFA between peri-tumoural adipose tissue against contralateral breast in patients. There were no significant differences in UBI, TRG, MUFA and PUFA between contralateral breast in patients against the average of both breasts in controls. There was a significantly higher disparity in UBI ($p = 0.0003$) in patients (0.28 ± 0.11) than controls (0.13 ± 0.08). There was a significantly higher disparity in TRG ($p = 0.012$) in patients (0.20 ± 0.15) than controls (0.08 ± 0.04). There were no significant differences in disparities in MUFA and PUFA between patients against controls.

Discussion/Conclusion: There was a greater imbalance in lipid unsaturated bond index and triglycerides in patients, and peri-tumoural lipid composition warrants further investigation towards a potential surveillance and early detection target for breast cancer.

Contact: g.cheung@abdn.ac.uk

Abstract number: O06

Peri-tumoural spatial distribution of lipid composition and tumour cellular differentiation in breast cancer

Sai Man Cheung[1], Kwok-Shing Chan[1], Nicholas Senn[1], Ehab Husain[2], Yazan Masannat[3], Steven D Heys[1], Jiabao He[1]

1. Institute of Medical Sciences, University of Aberdeen
2. Pathology Department, Aberdeen Royal Infirmary
3. Breast Unit, Aberdeen Royal Infirmary

Background: Peri-tumoural lipid composition is key to early detection of breast cancer, since a deregulation of lipid composition in adipose tissue is shown to precede cancer development. Novel method of chemical shift-encoded imaging allows rapid mapping of entire breast, enabling the quantification of spatial distribution of lipid composition. We hypothesise that peri-tumoural spatial distribution of lipid composition is sensitive to tumour cellular differentiation, and is associated with tumour proliferative activity.

Methods: Twenty whole tumour specimens freshly excised from patients with invasive ductal carcinoma (9 Score 2 and 11 Score 3 in tubule formation) were scanned on a 3 T clinical scanner (Achieva TX, Philips Healthcare). The maps of the number of double bonds in triglycerides were computed from chemical shift-encoded imaging, before subsequent calculation of quantitative maps of polyunsaturated fatty acids (PUFA), monounsaturated FA (MUFA) and saturated FA (SFA) as a percentage of the total amount of lipids. The spatial distribution (mean, skewness, entropy and kurtosis) was computed based on histogram distribution for each lipid constituent. The proliferative activity marker Ki-67 was assessed histologically.

Results: For MUFA, there were significant differences between groups in mean ($p = 0.01$), skewness ($p = 0.01$), entropy ($p = 0.02$), kurtosis ($p = 0.04$), and correlations against Ki-67 in mean ($\rho = -0.54$), skewness ($\rho = 0.60$) and entropy ($\rho = 0.67$), but not in kurtosis. For SFA, there were significant differences between groups in mean ($p = 0.03$) and skewness ($p = 0.01$), and correlation against Ki-67 in mean ($\rho = 0.59$). For PUFA, there was no significant difference in mean, skewness, entropy or kurtosis between the groups.

Discussion/Conclusion: There was an association between peri-tumoural spatial distribution of lipid composition with tumour cellular differentiation and proliferation. Peri-tumoural lipid composition imaging might have potential in early detection of breast cancer.

Contact: g.cheung@abdn.ac.uk

Abstract number: O07

Are baseline mammographic and ultrasound features associated with metastasis free survival in women receiving neoadjuvant chemotherapy for invasive breast cancer?

Andy Evans[1], Yee Ting Sim[2], Patsy Whelehan[2], Sarah Savaridas[2], Lee Jordan[2], Alastair Thompson[3]

1. Dundee University
2. Breast Unit Ninewells Hospital, Dundee
3. Baylor College of Medicine, Houston, Texas

Objectives: To identify associations between baseline ultrasound (US) and mammographic features and metastasis free survival (MFS) in women receiving neo-adjuvant chemotherapy (NACT) for breast cancer.

Methods: The data were collected as part of an ethically approved prospective study. Women with invasive breast cancer receiving NACT who were metastasis free at diagnosis were included. Baseline US and mammography were performed. Imaging was assessed by an experienced breast radiologist who was blinded to outcomes. US imaging features documented included posterior effect, skin thickening, size and stiffness using shear wave elastography (SWE). The mammographic features documented were spiculation and microcalcification. The development of metastatic disease was ascertained from computer records. Statistical analysis was performed using Kaplan Meier survival curves and Receiver Operator Characteristic (ROC) analysis.

Results: 171 women with 172 cancers were included in the study and 55 developed metastatic disease. Mean follow-up was 6.0 years. Women with mammographic calcification had significantly poorer metastasis free survival (MFS) compared to women without calcification (p=0.043, 6 yr MFS 50% vs 69%). Women bearing cancer with distal shadowing had poorer MFS than women without shadowing (p=0.025, 6 yr MFS 47% vs. 73%). Women with US skin thickening had poorer MFS compared to women without skin thickening (p=0.032, 6yr MFS 52% vs. 68%). Mammographic spiculation, US size and stiffness at SWE had no significant association with MFS.

Conclusion: We have identified mammographic and US features associated with MFS in women receiving NACT. Such information may be useful when counselling patients about the benefits and risks of NACT.

Acknowledgements: We would like to thank SINAPSE for funding from their Innovation Partnership Fund.

Contact: a.z.evans@dundee.ac.uk

Abstract number: O08

Is skin thickening and enhancement on breast MRI associated with metastasis-free survival (MFS)?

Valentine Mberu[1], Jennifer Macfarlane[2], E. Jane Macaskill[3], Andrew Evans[1]

1. University of Dundee, School of Medicine, Ninewells Hospital
2. Medical Physics, Ninewells Hospital, NHS Tayside
3. Breast surgery department, Ninewells Hospital, NHS Tayside

Introduction: Given the increased use of neoadjuvant chemotherapy, pre-operative predictors of survival become useful. The aim of this project was to identify associations between the skin thickening and enhancement on MRI with metastasis-free survival (MFS). This association has not previously been investigated.

Method: Interrogation of a prospectively collected database of ultrasound visible breast lesions showed 168 lesions with pre-treatment MRIs available for analysis. Retrospective review was performed blinded to outcome. Factors recorded were presence of skin thickening and enhancement as well as mass characteristics (focality, size, shape, margin, enhancement curve type and pattern), presence of non-mass enhancement (NME), perilesional oedema, background parenchymal enhancement and presence of abnormal nodes. Statistical analysis used Chi-squared test, Kaplan-Meier survival curves, Receiver-Operator Characteristic (ROC) curves and Cox-proportional hazards regression.

Results: During an average follow-up period of 5.9 years, 15 patients developed metastases. Patients with skin thickening [18 of 23 (78%) vs 135 of 145 (93%), p= 0.024] and skin enhancement [13 of 17 (76%) vs 140 of 151(93%), p=0.0358] were associated with poorer MFS. In addition, large index lesion size [$p < 0.001$, AUC 0.859], large sum of all masses [$p < 0.001$, AUC 0.834], increasing total lesion extent include NME [$p < 0.001$, AUC 0.763] and abnormal axillary nodes [42 of 50 (84%) vs 111 of 118 (94%), p=0.0210] were also associated with poor MFS. Multivariate analysis was attempted but was unsuccessful due to the small number of events.

Conclusion: In additional to well-known prognostic factors such as lesion size and presence of abnormal nodes, skin thickening and enhancement is associated with poor MFS. This knowledge may be helpful when discussing the appropriateness of neoadjuvant therapy with patients.

Contact: v.k.mberu@dundee.ac.uk

Abstract number: O09

Scotland's First MR Guided Focused Ultrasound Surgical Treatment

T. Brunton[1], F. Cossor[4], G. Frazzetta[4], K. Ibrahim[2,3], B. Jagpal[1,2], A.K. Kanodia[1], S. Khan[3], **J. A. Macfarlane[1]**, J. MacKay[1], G Mackenzie[1], N. McSorley[1], C. Mutch[1], G. Prasad[1], **I.** Schmidt[4], J. D. Steele[2], A. Taylor[1], B. Uylatt[1], T. Gilbertson[1]

1. NHS Tayside
2. University of Dundee
3. Department of Clinical Neurosciences, NHS Lothian
4. InSightec

In a joint collaboration between NHS Tayside and the University of Dundee, a Neuro Exablate system (InSightec, Israel) has been installed on 3T PrismaFIT (Siemens, Germany). Supported by InSightec, the first treatment was delivered in June 2021 by a multi-disciplinary team.

For patients with medically retractable Essential Tremor, the current surgical option is the implantation of Deep Brain Stimulation (DBS) electrodes. MRgFUS permits an incisionless alternative.

A 66 year-old male with Essential Tremor successfully underwent right sided VIM thalamotomy via ablation. Low power sonications and MR temperature mapping were used to refine the target site and volume, informed by repeated neurological examinations to assess the patient's response. Significant transient improvement in tremor confirmed the target volume. Higher power sonication was then deployed to create an irreversible lesion. The patient was on the bed for 3 hours. An immediate therapeutic effect was achieved. An MRI scan performed the following morning demonstrated the focal lesion in the right VIM thalamic nucleus with minimal surrounding oedema.

Our installation is the second of its kind in the UK and the first in Scotland. Treatment was made possible by a team which included Neurosurgery, Neurology, Radiography, Neuroradiology, Medical Physics, Anaesthetics, Psychiatry, and those who support them.

Contact: Jennifer.Macfarlane@nhs.scot

Abstract number: O10

Segmentation of Thalamic Nuclei for Targeting MR Guided Focused Ultrasound Surgery

Graeme G. Mackenzie[1], Jennifer A. Macfarlane[2], Douglas J. Steele[3], Tom Gilbertson[1]

1. Department of Neurology, Ninewells Hospital & Medical School, Dundee, UK
2. Division of Imaging Science and Technology, Medical School, University of Dundee, Dundee, UK
3. NHS Tayside Medical Physics, Ninewells Hospital, Dundee, UK

Introduction: Dundee University has recently installed Exablate Neuro (Insightec) MRgFUS equipment in the Ninewells 3T PRISMAFIT (Siemens) scanner. The surgical target for essential tremor (ET) is the ventral intermediate nucleus (VIM) of the thalamus. However, a recent report suggested the optimal target may be slightly more inferior and posterior. The targeting procedure starts at a default pre-defined stereotactic location which is then optimised over a period of hours on an individual patient basis. Here we compared the default starting location with the VIM.

Methods: MRI was acquired for pre-operative planning. 1 mm isotropic fluid and white matter suppressed images acquired from a FLAWS2 sequence were spatially normalised in SPM to Montreal Neurological (MNI) Space. Thalamic nuclei were segmented3 to obtain three dimensional volumes of thalamic nuclei including the VIM. The default starting location is three-quarters of the distance between the anterior and posterior commissure (AC, PC) posterior to the AC and lateral by 14 mm. This was compared with the VIM location.

Results: The default starting location was found to be slightly posterior and inferior to the VIM.

Discussion: The default starting location for MRgFUS treatment of ET is not the final location that is ablated so it's possible that the final lesions for patients will be in the VIM or closer to it. However, it is notable that a previous study found the optimal lesion location slightly posterior and inferior to the VIM.1 Development of this technique is expected to allow refinement of the default starting location and therefore shorter MRgFUS treatment sessions.

Contact: Graeme.Mackenzie3@nhs.scot

Abstract number: O11

Examining Cognitive Aspects of Relevance Judgement

Zuzana Pinkosova[1], William McGeown[1], Yashar Moshfeghi[1]

1. University of Strathclyde

Understanding relevance is an essential aspect of information seeking (Mizzaro, 1997; Saracevic, 2007; Schamber & Eisenberg, 1988). Through the interaction with relevant information, users can satisfy information needs and achieve their search task goal. However, what is considered relevant is subjective and dependent on the specific user mind state. Recent brain imaging research (i.e. Allegretti et al., 2015; Moshfeghi et al., 2013; Moshfeghi & Pollick, 2018) has significantly contributed towards the understanding of relevance by directly investigating a user's subjective perception of retrieved information. However, relevance has been operationalised as a whole, and its cognitive, affective or/and situational aspects (Saracevic, 2007) have not been examined. This work aims to explore the link between the cognitive aspects of relevance and the user's relevance perception.

We hypothesise that participants' relevance judgements will differ significantly based on their previous knowledge. This is based on previous findings suggesting that brain activation differs during the integration of incoming information due to what is already known, compared to unknown (Maguire, Frith and Morris, 1999). The findings might provide support for the cognitive relevance concept (Saracevic, 2007) and help to identify distinct cognitive processes underlying relevance perception.

In this study, participants engaged in a Question Answering Task, while their brain activity was recorded using an electroencephalogram (EEG) during the relevance judgement task. We examine the effect of previous knowledge on participants' subjective relevance judgements by gathering physiological and behavioural signals.

The present study extends previous brain imaging research, by investigating complex cognitive aspects of relevance. This study is the first to incorporate relevance theory and a neuroscience approach to investigate the neural correlates of cognitive states underlying relevance assessment. Better understanding of cognitive relevance might lead to the improvement of user-system interaction, increased search success and an improvement of information systems (Moshfeghi, Triantafillou, and Pollick, 2019).

Contact: zuzana.pinkosova@strath.ac.uk

Abstract number: O12

Developing advanced imaging as a tool for precision medicine in The Living Laboratory

Kristin E. Flegal

College of Medical, Veterinary & Life Sciences, University of Glasgow

A bid led by the University of Glasgow for UK Research and Innovation's flagship Strength in Places Fund (SiPF) was awarded £38M last year to create a global centre of excellence for Precision Medicine integrated within the Queen Elizabeth University Hospital campus. The SiPF Living Laboratory programme is focused on translating research innovation, from fields such as genomics, medical imaging and artificial intelligence, into clinical practice for the benefit of patients. Its aims are to improve health outcomes, drive economic development in Glasgow, and deliver savings for the NHS. Three exemplar projects within this 5-year programme are based at the Imaging Centre of Excellence (ICE) and delivered by consortia in a 'triple helix' approach of industry, academia and the NHS working alongside each other. A *coil development* project will develop and commercialise new 7T MRI RF coil designs, to establish a dedicated path to market for high-value coil manufacturing and facilitate the adoption of ultra-high field MRI into clinical use. A *radiogenomics* project will advance novel AI methods that harness information about early disease processes from imaging and utilise genomic data to enhance these weak signals, and will test the value of that precision diagnostics approach in oncology disease pathways. An *image analysis* project will establish an advanced image analysis facility at ICE to leverage Scotland's existing skills in medical imaging data analysis, distributed across the SINAPSE network, into a centralised commercial entity. This presentation will review initial progress in the three advanced imaging exemplar projects contributing to the Living Laboratory and identify opportunities for input and collaboration.

Acknowledgements: The Living Laboratory programme has received £38M funding from the Strength in Places Fund, £22M of support from industry partners and an additional investment of £27.5M from Glasgow City Region City Deal and Glasgow City Council. Partners on the three advanced imaging exemplar projects are the University of Glasgow, NHS Greater Glasgow & Clyde, Canon Medical Research Europe Ltd, MR CoilTech Ltd, and Siemens Healthineers.

Contact: kristin.flegal@glasgow.ac.uk

Abstract number: O13

Automated brain tumour identification using magnetic resonance imaging: a systematic review and meta-analysis

Omar Kouli[1,2], Ahmed Hassane[3], Kismet Hossain-Ibrahim[4], Douglas Steele[1]

1. Division of Imaging Science and Technology, Medical School, University of Dundee, Dundee, UK
2. Queen Elizabeth University Hospital, NHS Greater Glasgow and Clyde, Glasgow, UK
3. Aberdeen Royal Infirmary, NHS Grampian, Aberdeen, UK
4. Department of Neurosurgery, Ninewells Hospital, Dundee, UK

Introduction: Brain tumours are associated with high morbidity and mortality. Early diagnosis and accurate tumour delineation are essential for treatment and surgical planning. Magnetic resonance images (MRI) can be processed using manual, semi-automatic, and fully automatic techniques. Significant work has been devoted to improving automated techniques over the past two decades to improve brain tumour diagnosis. We aimed to provide a critical appraisal of the different automated techniques used in both brain tumour detection and segmentation to date and evaluate their diagnostic accuracy.

Methods: In this systematic review and meta-analysis, we searched MEDLINE, Scopus and Web of science for studies published from Jan 1, 2000, to May 8, 2021. The primary objective is to assess the diagnostic accuracy of the different automated techniques, including assessing potential biases and calculating combined estimates of sensitivity, specificity, area under the curve and Dice coefficient. The secondary objective is to review the MRI databases, modalities, tumour type, feature extraction and validation techniques utilised.

For detection techniques, binary diagnostic accuracy data were extracted, and contingency tables were constructed. Pooled SEN and SPE with 95% confidence intervals for will be calculated. A unified hierarchical model that was developed for the meta-analysis of diagnostic accuracy studies and plotted summary receiver operating characteristic (ROC) curves. For segmentation techniques, Dice coefficients were pooled, and weighted mean Dice coefficients were calculated. This study is registered with PROSPERO, CRD42021247925.

Conclusion: Our search identified 3,197 studies, of which 166 studies were included. To best of knowledge, this study is the first and largest systematic review and meta-analysis in this area. It aims to give an overview of the various segmentation/detection techniques and aid researchers identify the successful methods for automated brain tumour identification.

Contact: okouli@dundee.ac.uk

Abstract number: O14

Joint multi-field T1 quantification for Fast Field-Cycling imaging identifies ischaemic stroke at magnetic field strength below 20 mT

Vasiliki Mallikourti[1], Oliver Maier[2], Markus Bödenler[2,3], Rudolf Stollberger[2,5], P. James Ross[1], Mary-Joan MacLeod[4], Hermann Scharfetter[2], Lionel M. Broche[1]

1. Aberdeen Biomedical Imaging Centre, University of Aberdeen, Aberdeen, UK
2. Institute of Medical Engineering, Graz University of Technology, Graz, Austria
3. Institute of eHealth, University of Applied Sciences FH JOANNEUM, Graz, Austria
4. Institute of Medical Sciences, University of Aberdeen, Aberdeen, UK
5. BioTechMed-Graz, Graz, Austria

Introduction: Fast Field-Cycling (FFC) imaging1 measures variations of T1 relaxation with the magnetic field strength, known as T1 dispersion, exploiting novel biomarkers that are invisible to other imaging modalities. Our aim is to characterise ischaemic strokes with FFC imaging. We also propose a purpose-made reconstruction method2 that exploits the high spatial redundancy of FFC images by using total generalised variation (TGV3) regularisation over all images, combined with a mono-exponential model of magnetisation behaviour to provide T1 maps directly.

Methods: 2 patients were scanned within 24-96 h of presentation using a field-cycled inversion recovery spin echo sequence with three to four evolution fields typically ranging from 0.2 T to 0.2 mT, 2 to 4 mm in-plane resolution, 290 mm FOV, 10 mm slice thickness, 16 to 24 ms TE and no averaging.

Multi-field T1 quantification was performed using the joint TGV regularisation algorithm after validation on simulated datasets, compared to a standard curve fitting approach. The position of the stroke in FFC was compared with CT and MRI images for validation.

Results: The TGV-based method showed significant improvements in visual appearance over all fields in simulated and patient images (Fig. 1). Patient images exhibited visible contrast at 20 mT and below. The infarct region measured by FFC corresponded with CT and 3T MRI images. The in-vivo T1 dispersion profiles for the stroke area differed from other brain tissues (Fig. 2).

Discussion: This is the first-ever in-vivo measurement of T1 dispersion of stroke, which was made possible by the joint TGV regularisation method (processing tool available online4), demonstrating the potential for low fields in stroke.

References:

1. Broche, L. M. et al. Sci. Rep. 9, 10402 (2019)

2. Bödenler, M. et al. Magn. Reson. Med. In print,

3. Knoll, F. et al. Magn. Reson. Med. 65, 480–491 (2011)

4. Maier, O. et al. J. Open Source Softw. 5, 2727 (2020)

Contact: s02vm1@abdn.ac.uk

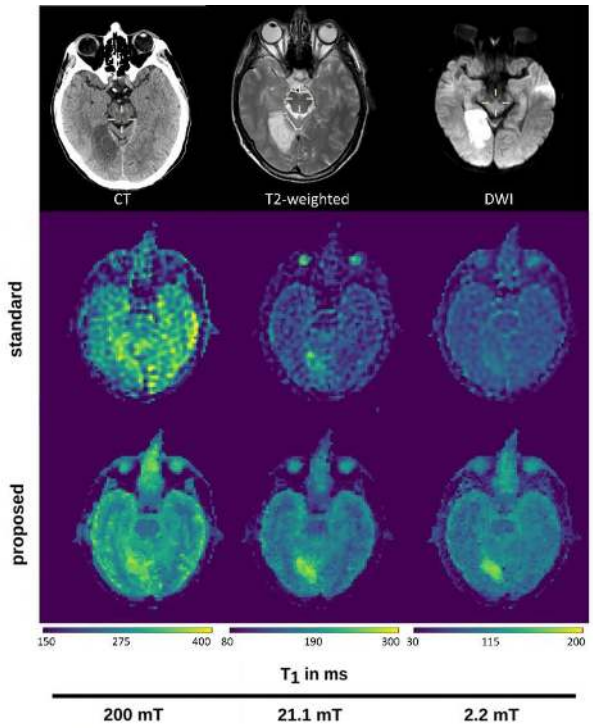

Figure 1. In vivo conventional imaging and multi-field T1 maps of a transverse slice of the brain of stroke patient I. CT, 3T T2-weighted, and diffusion weighted image (DWI) MRI (top row). T1 maps were obtained at three different evolution fields (200, 21.1, 2.2) mT by pixel-wise fitting of the signal model for each evolution field separately (middle row) and by the proposed multi-field model-based reconstruction approach utilising the joint information of all three evolution fields (bottom row).

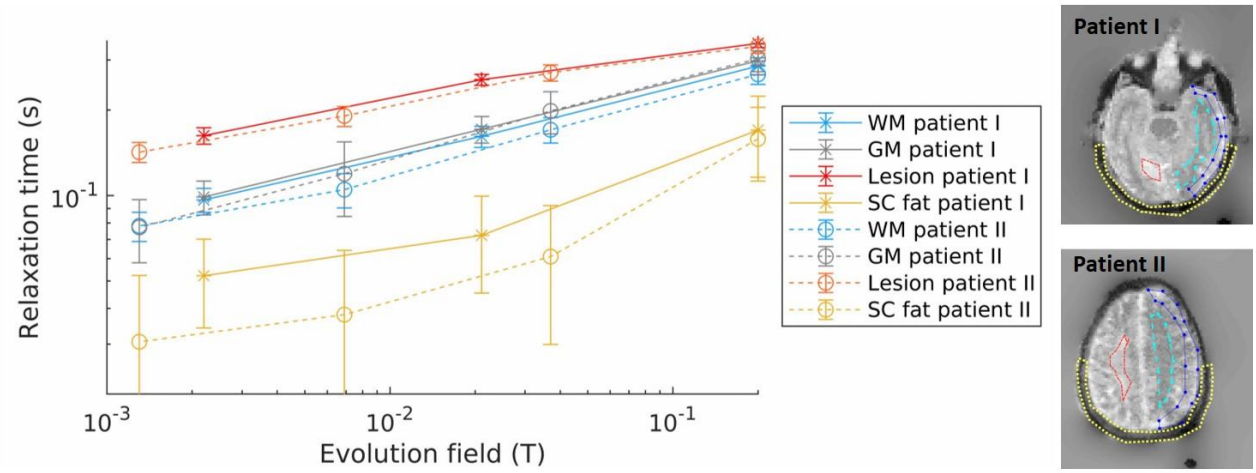

Figure 2. T1 dispersion profiles obtained from the patients I (solid lines) and II (dashed lines). The regions included subcutaneous fat (SC fat, yellow) measured between the scalp and the brain, grey matter (GM, grey) measured over two centimetres of the cortical region, white matter (WM, blue) measured over the inner region of the lobes and the lesion (red). The error bars stand for twice the standard deviation of the T1 values measured across the ROIs.

Abstract number: O15

Eigenvector alignment: Assessing functional network changes in Alzheimer's disease

Ruaridh A Clark[1], Niia Nikolova[2], Malcolm Macdonald[1], William J McGeown[3]

1. Electronic & Electrical Engineering, University of Strathclyde
2. Centre for Functionally Integrative Neuroscience, Aarhus University
3. School of Psychological Sciences & Health, University of Strathclyde

Functional connectivity networks for resting-state functional magnetic resonance imaging offer fundamental insights into the organisation of the human brain, as well as hypothesised disconnectivity effects in neurological brain disorders. There are a variety of analytic approaches to isolate and assess connectivity networks, such as independent components analysis, as well as graph-based methods for assessing features such as centrality. We present Eigenvector Alignment as a complementary method for assessing the functional alignment of brain regions, which mitigates against individual variations in functional connectivity by holistically evaluating all connections. This technique emerges from the study of complex networks, where embedding a network in a Euclidean space defined by the system's eigenvectors reveals node alignment and influence [1].

Our initial study of 10 healthy control, 10 probable Alzheimer's disease (AD) diagnosis, and 10 mild cognitive impairment (aMCI) subjects demonstrated that Eigenvector Alignment recognises the strength of bilateral connectivity in cortical areas of healthy control subjects, but also reveals degradation of this commissural system in those with (AD) [2]. Surprisingly little change in network structure is detected for key regions in the Default Mode Network, despite significant declines in the functional connectivity of these regions. In contrast, regions in the auditory cortex display significant alignment changes that begin in aMCI and are the most prominent structural changes in the functional networks of those with AD. Alignment differences between aMCI and AD subjects are detected, including notable changes to the hippocampal regions. Further analyses utilising Eigenvector Alignment will be presented using a larger rs-fMRI dataset available via the Alzheimer Disease Neuroimaging Initiative (http://adni.loni.usc.edu/).

1. Clark, Ruaridh A., et al. "Network communities of dynamical influence." Scientific reports 9.1 (2019): 1-13.

2. Clark, Ruaridh A., et al. "Eigenvector alignment: Assessing functional network changes in amnestic mild cognitive impairment and Alzheimer's disease." PloS one 15.8 (2020).

Contact: ruaridh.clark@strath.ac.uk

Abstract number: O16

Efficiency of marking and rendering software for epilepsy surgery

Mateo Gregory[1], Jose Bernal[2], Maria Trujillo[1], Alejandro Herrera[3]

1. Universidad del Valle, Cali, Colombia
2. The University of Edinburgh, Edinburgh, UK
3. Centro Médico Imbanaco Quirón Salud, Cali, Colombia

Epilepsy is one of the most common neurological diseases, affecting 50 million people worldwide. Approximately a third of all patients cannot be treated with antiepileptic drugs; in these cases surgical interventions are the most effective alternative. After resecting the epileptogenic tissue, surgeons mark it with biological dyes and place it in fixative solutions for storage and analysis. However, the tissue morphology varies over time, making physical annotations unreliable. Digital markings on magnetic resonance images (MRI) during pre-surgery planning may be considered complementarity to improve spatial reference and subsequent histopathological evaluations. In this work, we evaluated software enabling the marking and rendering of pre-surgical MRIs. First, we searched systematically for applications to segment and visualise 3D medical images. We found 17 that met the search criteria, but only three of them were free, open-source and cross-platform, and supported Dicom and nifty formats: MITK, ITK-Snap, and 3DSlicer. Second, we assessed how usable each of these applications was using the "thinking aloud" usability tool. For that, we asked seven senior medicine and computer science students to segment regions of interest in MRIs using the three applications, measured the time it took them to perform these tasks and counted the number of errors they made overall. Despite the complexity of its interface, most users committed the least amount of errors in MITK and spent the least amount of time in 3DSlicer (average time [min]: MITK 18.7; ITK-Snap 21.6; and 3DSlicer 17; total errors: MITK 120; ITK-Snap 199; 3DSlicer 199). Most errors with MITK and 3DSlicer occurred during its exploration and not during the segmentation per se, as opposed to those with ITK-Snap. This preliminary work suggests that MITK and 3DSlicer are suitable for digital marking but further testing with surgeons and histopathologists is needed to determine its applicability in epilepsy surgery.

Acknowledgements: JB holds an MRC Precision Medicine Doctoral Training Programme studentship from the University of Edinburgh, University of Glasgow, and Medical Research Council (Award reference 2096671)

Contact: mateo.gregory@correounivalle.edu.co

Abstract number: O17

Measurement of microbubble backscattering signals in 3D-printed, physiologically-relevant platforms

Roger Domingo-Roca[1], Mairi E. Sandison[1], Richard O'Leary[2], Joseph Jackson-Camargo[2], Helen E. Mulvana[1]

1. Department of Biomedical Engineering, University of Strathclyde
2. Department of Electronic and Electrical Engineering, University of Strathclyde

Systemically injected microbubbles (MBs) are used to enhance contrast, target, and aid drug delivery in conjunction with ultrasound. Microbubbles present highly nonlinear behaviour even when driven at low mechanical indices (MI, which relate the frequency and the peak negative pressure of the driving ultrasonic signal). These nonlinear oscillations have the ability to generate bioeffects that can be monitored and exploited to enhance permeabilization and extravasation, becoming useful for disease treatment. The amount and extent of these effects depends on a set of physical and biological parameters (ultrasound characteristics, flow rate, channel diameter) that can be controlled to better understand how MBs scatter sound. In regions of quasi-quiescent flow, buoyancy will take MBs closer to the vessel walls, where their oscillation dynamics will play an important role in generating bioeffects (similarly to highly confined MBs). Contrarily, MBs in central regions of large diameter channels will displace larger volumes of fluid but generate less relevant bioeffects. How can we know, then, where MBs are and how they behave? Changes of MI, flow rate, and channel diameter will all influence MBs dynamics, leaving a characteristic fingerprint that can be measured by analysing the ultrasound signal backscattered by MBs. We have developed a fully 3D-printed system, using tissue-mimicking hydrogels, showing accurate replication of physiologically-relevant morphologies. We connected these microchannels to a syringe pump (to control the flow rate of the MBs, added as bolus) and placed them at the focal point of two transducers (f=3.5 MHz, Panametrics, acting as a transmit and receive, respectively) in a tank of outgassed water. Control of flow rate (0 - 50 µL/min), microchannel diameter (200 - 500 µm), and MI (0.15 - 0.45) result in characteristic backscattered signals that provide fundamental information about MBs activity, which is extremely important towards clinical application of ultrasound-based therapies.

Acknowledgements: The authors would like to thank the Centre for Ultrasonic Engineering, especially to Dr. Charles McLeod and Euan Foster, for their support with technical equipment. This research was conducted under the Biotechnology and Biological Sciences Research Council (BB/T01202/1).

Contact: roger.domingo-roca@strath.ac.uk

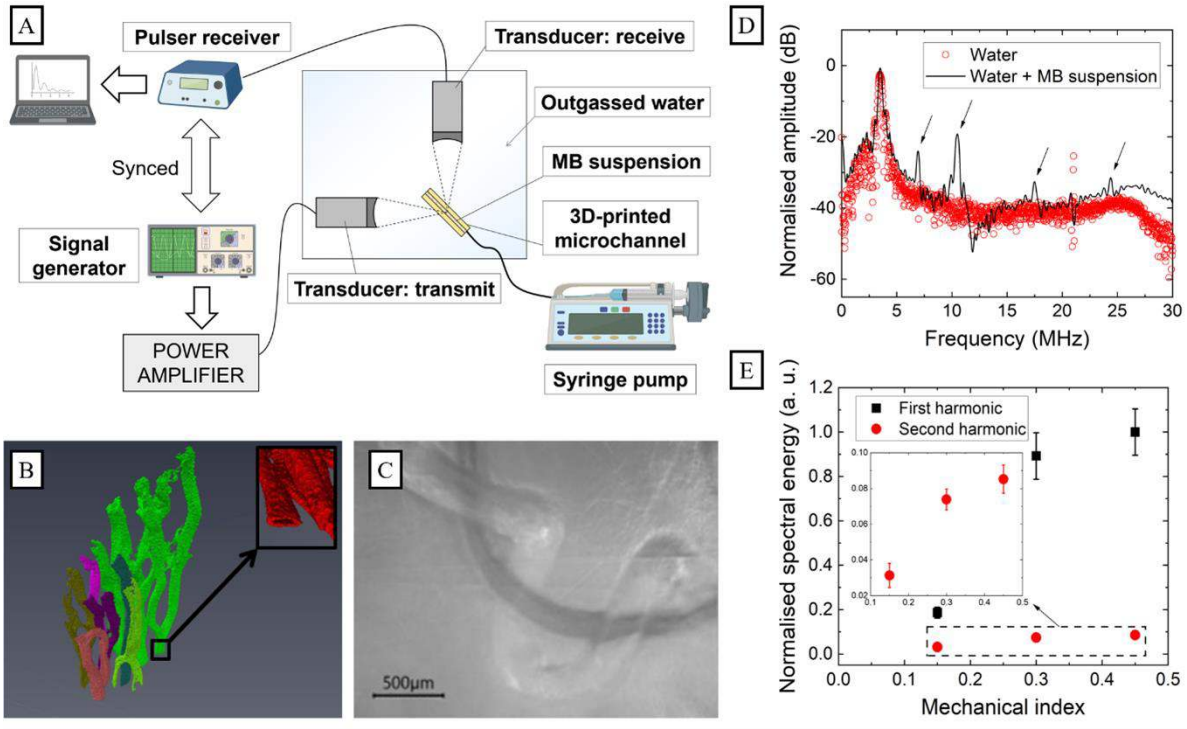

Figure 1.

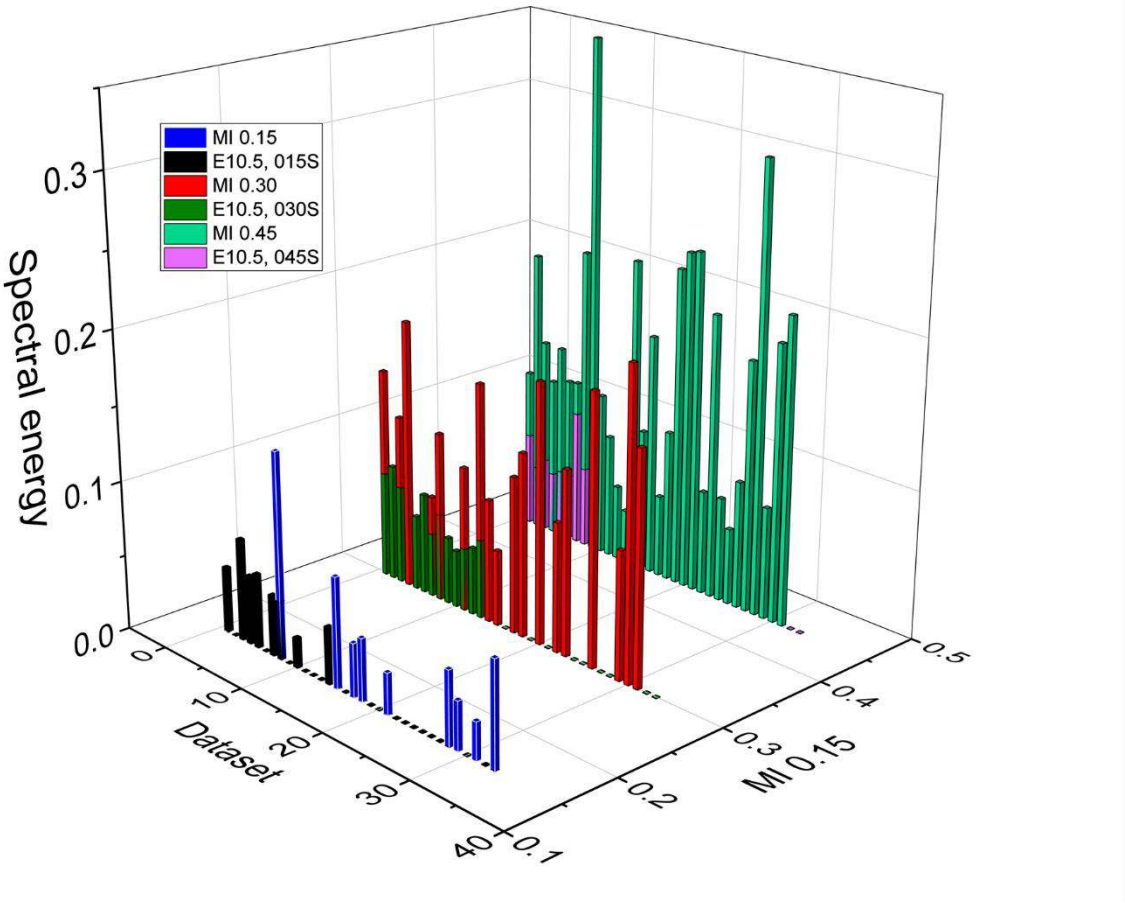

Figure 2.

Abstract number: O18

Direct imaging of glymphatic transport using H217O MRI

Mohammed S. Alshuhri[1], **Alaa Alghanimy**[1], Lindsay Gallagher[1], Lorraine Work[1], William M. Holmes[1]

1. Glasgow Experimental MRI Centre (GEMRIC), Institute of Neuroscience and Psychology, University of Glasgow

Introduction: The recently proposed glymphatic pathway for solute transport and waste clearance from the brain has been the focus of intense debate. By exploiting an isotopically enriched MRI tracer, H217O, we directly imaged glymphatic water transport in the rat brain in vivo for the first time. Moreover, we confirm the critical role of aquaporin-4 channels in glymphatic transport.

Methods and Materials: Study 1) MRI was used to image glymphatic transport in male Wistar rats, via intracisternal infusion (1.8 µl/min) of; Gd-DTPA (n=7) with T1 weighted imaging; and 90% 17O-enriched water H217O (n=7) with high SNR T2 weighted 1H imaging. Study 2) To test the role of AQP4 in glymphatic transport, an AQP4 inhibitor (TGN-020) was administered intraperitoneally (200mg/kg in 5 ml) 15 min before starting the MRI. For both studies, MRI images of the rat brain were dynamically acquired for 85 minutes. Study 3) to test the effect of the AQP4 facilitator (TGN-073) on the glymphatic flow, rats were randomly assigned to either drug or vehicle groups. IP injection of either TGN-073 or the vehicle (200 mg/kg in 20ml/kg body weight) was administered 30 mins before starting the MRI. For both studies, Physiological parameters and arterial blood gas analysis were continuously monitored.

Results: Our H217O results reveal glymphatic transport that is dramatically faster and more extensive than previously seen using Gd-DTPA, and unlikely to be explained by diffusion alone (see Figure 1). In the group treated with the AQP4 inhibitor (TGN-020), there was a 80% (± 10%) reduction in H217O transported into the parenchyma compared with the vehicle group (see Figure 2). Moreover, rats treated with TGN-073 showed more extensive distribution of H217O and higher parenchymal uptake compared with the vehicle group (see Figure 3). Both results confirm the critical role of AQP4.

Conclusion: We have conclusively demonstrated that glymphatic flow imaged using our H217O tracer is much more rapid and extensive than when imaged using the Gd-DTPA. This is strong evidence that the interstitial fluid experiences a substantial bulk flow, which can more rapidly clear waste molecules from the parenchyma than by diffusion alone. Further, we were able to conclusively demonstrate that these glymphatic flows are strongly mediated by AQP4. Further, since glymphatic impairment due to AQP4 dysfunction is potentially associated with several neurological disorders such as AD, dementia and traumatic brain injury, enhancing AQP4 functionality using AQP4 facilitator (TGN-073) might be a promising therapeutic target.

Contact: 2502242A@student.gla.ac.uk

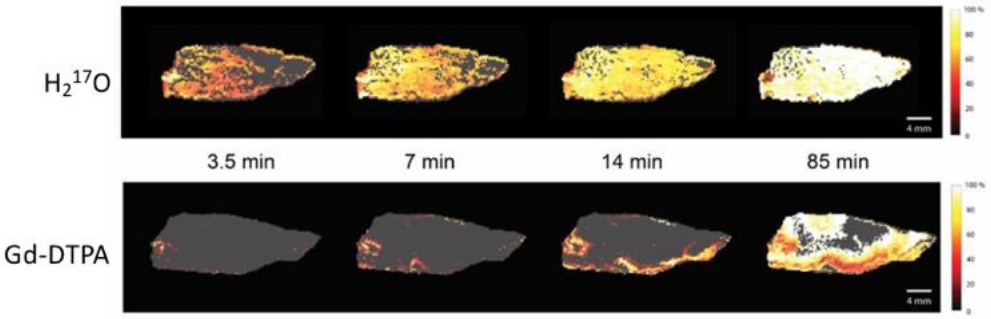

Figure 1. Representative sagittal MRI demonstrating the temporal evolution of tracer over 85 min of recording.

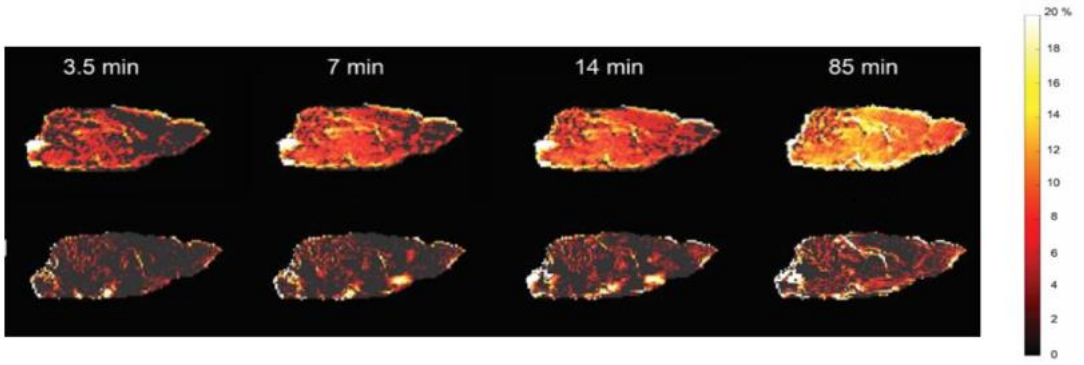

Figure 2. Serial sagittal MRI revealing the temporal evolution of H217O tracer for vehicle-treated rats (upper panel, n=6), and rats treated with the AQP4 inhibitor, TGN 020, (lower panel, n=6).

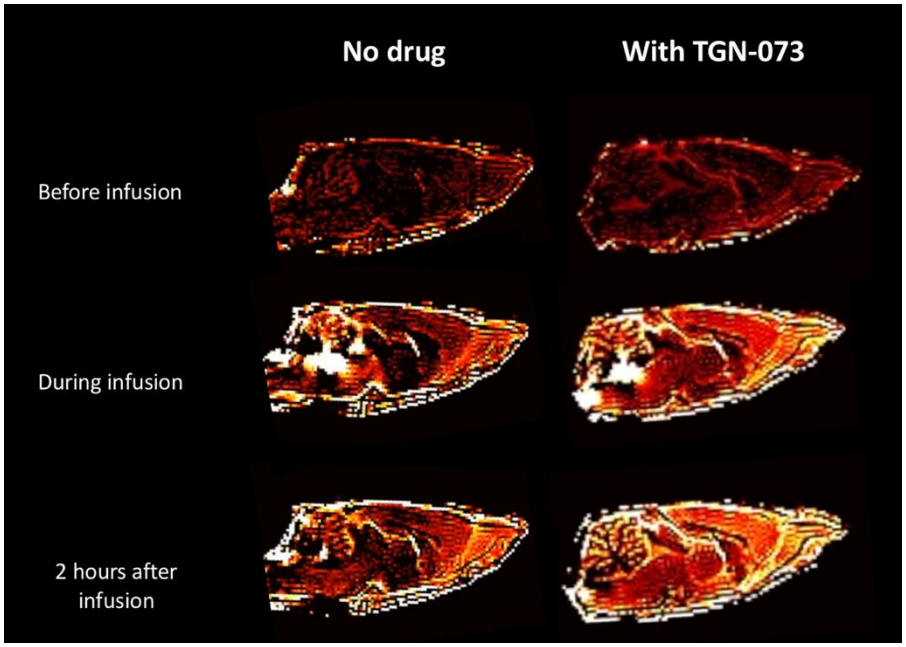

Figure 3. MRI of the glymphatic flow using $H_2{}^{17}O$ as an exogenous contrast

Abstract number: O19

Comparison of [18F]MNI-1038 (racemate) and [18F]MNI-1126 (R-enantiomer) kinetics in the mouse brain

Catriona Wimberley[1,2], Carlos J. Alcaide-Corral[2,3], Timaeus E. F. Morgan[2,3], Holly McErlain[4], Theresa Wong[1], Euan B. McLean[4], Seth Grant[1], Andrew Sutherland[4], Adriana A. S. Tavares[2,3]

1. Centre for Clinical Brain Sciences, University of Edinburgh
2. Edinburgh Imaging, University of Edinburgh
3. BHF-University of Edinburgh Centre for Cardiovascular Science, University of Edinburgh
4. School of Chemistry, University of Glasgow

Introduction: A recent target of interest for PET imaging has been the synaptic vesicle protein 2A (SV2A) which is thought to be an indicator of synaptic density. Severa lradiotracers have been developed for imaging SV2Awith PET, the most prominent is[18F]MNI-1126, which is the R-enantiomer of [18F]MNI-1038.Although the kinetics of these two compounds have been assessed in non-human primates, there is no data available on the performance of both compounds in the mouse. This project aimed to compare kinetic properties of [18F]MNI-1038 (racemate) and [18F]MNI-1126(R-enantiomer) in the mouse brain.

Methods: Eight male C57Bl6/J mice (15±1.6weeks, 29±1.6g) underwent dynamic PET scanning for 2 hours following administration of [18F]MNI-1038(13±4.8MBq, n=4) or[18F]MNI-1126 (16±7.0Mbq, n=4). The reconstructed PET images were summed from 30 to 60 minutes and maps of the standard uptake value (SUV)were generated (Sadasivam et al.2020). An MRI based mouse brain atlas was registered to the PET scans, regional SUVs were extracted and a correlation performed between the two compounds.

Results: Figure 1 shows the average maps for [18F]MNI-1038(racemate, (a)) and[18F]MNI-1126 (R-enantiomer, (b)) and the whole brain time activity curves (TACs, (c)). The SUV maps (30-60 minutes) show a similar spatial distribution but the [18F]MNI-1038 SUV is lower over the whole brain. Despite the lower values, the regional SUVs are highly correlated (r=0.88, p= 1.33e-18).

Conclusion: [18F]MNI-1038 and [18F]MNI-1126 showed similar uptake distribution throughout the brain, although the pure enantiomer compound shows a higher SUV profile. The TACs showed that more of the pure enantiomer sample enters the brain tissue than from the racemic mixture sample. Further studies should be conducted to investigate the kinetic parameters of both samples, as well as the metabolic profile in blood and brain tissue.

Acknowledgements: This project is funded by the Wellcome Trust, TDA 221295/Z/20/Z

Contact: catriona.wimberley@ed.ac.uk

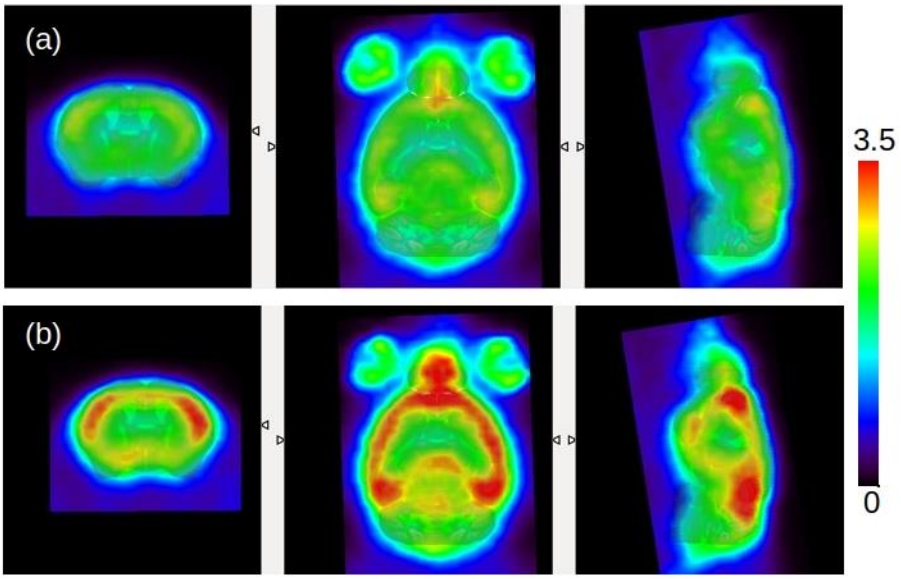

(c) Average SUV curves

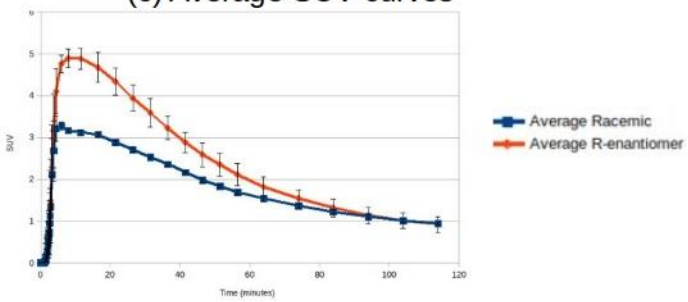

Abstract number: O20

Mesoscopic imaging of pediatric palatine tonsil infection

Megan Clapperton[1], Jordan Murray[1], Catriona Douglas[2], Gail McConnell[1]

1. Department of Physics, SUPA, University of Strathclyde, 107 Rottenrow, Glasgow, G4 0NG
2. Department of Otolaryngology, Head and Neck Surgery, Queen Elizabeth University Hospital, 1345 Govan Road, Glasgow, G51 4TF

Recurring paediatric tonsilitis is one of the most common problems presented to GPs in the UK, with an annual reported incidence of 37 per 1000 population [1]. Recurring tonsillitis has detrimental effects on children's quality of life. Often, antibiotic treatment of the infection does not suffice and if a patient has seven or more cases of tonsillitis per year the complete removal of the tonsils is recommended [2].

Studies of tonsillitis infections have been performed previously by Chloe and Faddis, showing the presence of gram-positive and gram-negative bacteria within the tonsil crypts, presenting the ultrastructural appearance of a biofilm matrix [3].

We report the first demonstration of mesoscopic imaging of bacterial infection of the palatine tonsil using the Mesolens. The Mesolens, developed at the University of Strathclyde, offers the unique combination of a low magnification (4x) and high numerical aperture (0.47) lens which has an imaging area of 6 mm x 6 mm. The Mesolens can resolve features as small as700nm laterally and 7um axially [4], this field of view means that the probability of detecting a few bacteria in the specimen is high.

Samples were collected via a swab from the surface of unfixed palatine tonsil tissue acquired via tonsillectomy at the NHS Royal Hospital for Children, Glasgow, which had been transported and stored in PBS for 2 hours before processing. Specimens were prepared using a standard Gram stain protocol. Figure 1 shows a colour brightfield Mesolens image a swab from the tonsil surface.

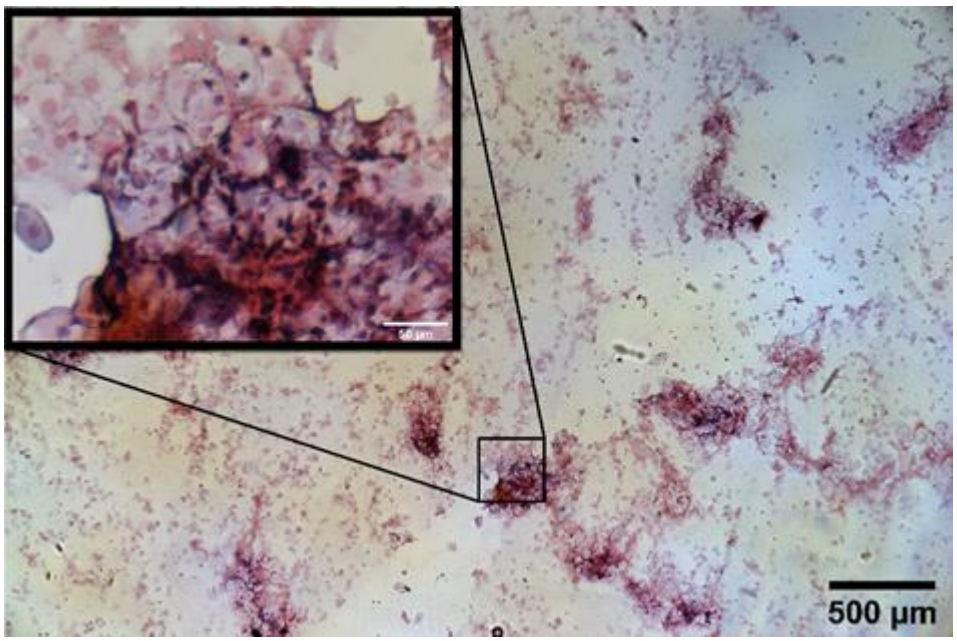

Using the Mesolens to study infection offers an advantage over conventional objective lenses. The large field of view and sub-cellular resolution throughout unlocks the possibility to understand the prevalence of

bacteria in larger specimens than can normally be studied with a light microscope, and any infection has a greater chance of being detected.

Contact: megan.clapperton@strath.ac.uk

Abstract number: O21

Towards Robust Real-World Decision Support for Skin Lesion Diagnosis

Jacob Carse[1], Tamas Suveges[1], Colin Fleming[2], Charlotte Proby[1,2] Emanuele Trucco[1], Stephen McKenna[1]

1. CVIP, School of Science and Engineering, University of Dundee
2. Dermatology, NHS Tayside

Skin lesion image analysis has great potential to improve diagnostic decision making and efficiency of clinical workflows in general practice and dermatology. A deployable decision support system needs to be able to ascertain when it is ill-equipped to recommend a diagnosis, either because images lack sufficient diagnostic information, or because of insufficient training examples. It should also account for the different costs associated with different misclassification errors. For example, deciding that a skin lesion is benign when it is in fact malignant is a more costly error than deciding it is malignant when it is benign. These factors are important for clinical translation; building classifiers that simply optimise measures such as mean class accuracy is clearly insufficient. This presentation reports progress towards selective, cost-sensitive, lesion image classifiers for deployment in real-world clinical settings. We used deep image classifiers, that produce well-calibrated class probability distributions and confidence measures, to make cost-sensitive recommendations when confidence is sufficiently high, while abstaining from making any recommendation for low-confidence images. We employed Bayesian deep learning, Monte Carlo dropout, Selective Net, and temperature scaling. We report experiments using the ISIC2019 challenge dataset as well as data from NHS Tayside Dermatology. We find that Bayesian deep learning can be effective in this cost-sensitive setting.

Acknowledgements: This report is independent research funded by the National Institute for Health Research (Artificial Intelligence, Deep learning for effective triaging of skin disease in the NHS, AI_AWARD01901) and NHSX. The views expressed in this publication are those of the authors and not necessarily those of the National Institute for Health Research, NHSX or the Department of Health and Social Care. This research was also funded by the Detect Cancer Early programme, and the Discovery Institute of Dermatology.

Contact: jcarse@dundee.ac.uk

Abstract number: O22

Strain estimation in aortic roots from 4D echocardiographic images using medial modelling and deformable registration

Peter Mortensen[1], Ankush Aggarwal[1], Jilei Hao[2], Lukasz Kaczmarczyk[1], Paul Yushkevich[2], Alison Pouch[2]

1. Glasgow Computational Engineering Centre, James Watt School of Engineering, University of Glasgow
2. Department of Radiology, University of Pennsylvania

Even though the central role of mechanics in cardiovascular system is widely recognized, estimating mechanical deformation and strains, in-vivo, remains a fundamental challenge. Herein, we present a semi-automated framework to estimate strains from four-dimensional(4D) echocardiography images and apply it to aortic root for patients with normal trileaflet aortic valve (TAV) and anomalous bileaflet aorticvalve (BAV).

The framework takes the geometries from the echocardiographs and creates a medial mesh, from which the strain estimations are taken. The method of strain estimation is based on fully nonlinear shell-based kinematics, which divides the strains into in-plane (shear and dilatational) and out-of-plane. As well as strains, several key values are also estimated with the framework. Notably, the root radius, the wall thickness and lumen volume. The framework also allows the movement of the root walls to be separated from the overall motion that caused by the movement of the heart.

The results indicate that even for size-matched aortic roots, patients with BAV experience larger regional shear strains in their aortic roots. This difference in strains might be a contributing factor to their higher risk of aneurysm development. The proposed framework will be made openly available and applicable to any tubular structures. Also, the BAV roots in general are larger than the TAV roots and have greater variation in their roots geometries. Another significant result is that these values are estimated over then entire cycle of the heartbeat, which is rarely recorded from in-vivo data. The moments at which the valves open and close is recorded allowing the cycles to be standardised and properly compared.

Acknowledgements: This work was supported in part by the Chan Zuckerberg Foundation and the Institute of Physics and Engineering in Medicine.

Contact: peter.mortensen@glasgow.ac.uk

Abstract number: O23

Quantitative Comparison of Arterial Spin Labelling Imaging Sequence in Ischaemic Stroke Patients: A Bland-Altman Analysis.

Zanariah Mohd[1,2], Keith Muir[1]

1. College of Medical, Veterinary and Life Sciences, University of Glasgow, United Kingdom
2. Faculty of Health Sciences, Universiti Teknologi MARA, Malaysia

Introduction: Arterial spin labelling (ASL) magnetic resonance perfusion imaging allows non-invasive quantification of cerebral blood flow (CBF) without contrast administration. However, not all clinical scanners were equipped with various ASL imaging sequence. Thus, we investigated the agreement between two common ASL sequences in the ischaemic stroke clinical cohort.

Method: Patients were part of a prospective, single-centre pilot observational study of late time window perfusion 4.5 to 24 hours after symptom onset. Patients who received revascularisation therapy were excluded. Pulsed ASL (PASL) and pseudo-continuous ASL (PCASL) imaging were acquired at 48 to 72 hours after stroke onset using a 3T MRI scanner. ASL images without calibration images were excluded from the analysis. ASL perfusion maps were post-processed using BASIL software pipelines which include motion correction and image registration. The post-processed perfusion maps were used to quantify the CBF in grey (GM) and white matter (WM). The Bland-Altman analysis was performed to quantify the agreement between CBF measured both by PCASL and PASL.

Results: In 26 patients, mean age 65±11 years and median National Institutes of Health Stroke Scale (NIHSS) of 3±7, ASL were acquired at median of 58 hours after symptom onset. The mean GM and WM CBF measured by PCASL were 39±11 ml/100g/min and 19±5 ml/100g/min, respectively. For PASL, the CBF for GM and WM measured were 46±13 ml/100g/min and18±7 ml/100g/min, respectively. For Bland-Altman analysis, the mean difference for GM is-7.37 ± 10.03 ml/100g/min, and the mean difference for WM is 1.29 ± 5.18 ml/100g/min. Almost all of the CBF measurements were within the 95% limits of agreement.

Discussion/Conclusion: Both PCASL and PASL provided reliable CBF measurement in ischaemic stroke patients. Various ASL imaging parameters should be considered to ensure accurate perfusion measurement.

Contact: 2307341z@student.gla.ac.uk

Abstract number: O24

68Ga-FAPI as a marker of fibrosis activity and matrix remodelling in patients with myocardial infarction

Anna Kate Barton[1], Evangelos Tzolos[1], David Newby[1], Marc Dweck[1]

1. Centre for Cardiovascular Science, The University of Edinburgh

Fibrosis is a fundamental process underlying almost all cardiomyopathic conditions. Established fibrosis can be detected by existing imaging techniques including cardiovascular magnetic resonance. However, these techniques are not specific for fibrosis and do not measure fibrosis activity or matrix remodelling, limiting our ability to detect early-stage disease and differentiate active from end-stage phenotypes. Fibroblast activation protein is key to fibrogenesis. It is expressed in the myocardium following myocardial infarction and in thin-capped fibroatheroma. Radiolabelled fibroblast activation protein inhibitor (68Ga-FAPI) measures in vivo fibrosis activity and matrix remodelling. We will investigate the timing and pattern of myocardial fibrosis activity following acute myocardial infarction using hybrid 68Ga-FAPI positron emission tomography, hypothesising peak fibrosis activity will occur within 2 weeks of acute myocardial infarction and will predict scar formation and cardiac remodelling. We will also assess matrix remodelling and fibrosis activity in aortic and coronary atheroma. We have performed 68Ga-FAPI PET/MR in 2 patients with acute ST-elevation myocardial infarction. In both patients imaged 3 and 8 days respectively following myocardial infarction, intense 68Ga-FAPI uptake was observed within the infarct zone (SUVmean 5.6 and 6.9) and demonstrated a >6-fold increase in activity compared to remote myocardium (SUVmean 0.9 and 0.8). The 68Ga-FAPI signal closely aligned with the pattern of injury observed on late gadolinium enhancement imaging. Increased 68Ga-FAPI uptake was also observed in the aorta and carotid artery (SUVmean 1.6). This project will enhance our understanding of fibrosis activity and matrix remodelling in myocardial infarction and unstable atherosclerotic plaque with potential application to a broad range of cardiovascular diseases.

Contact: abarton3@ed.ac.uk

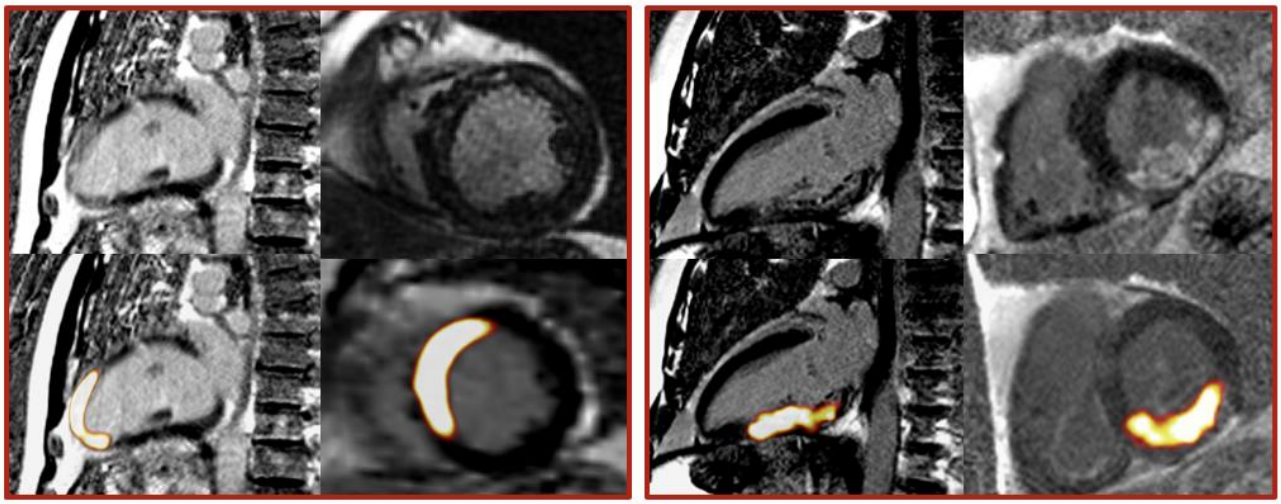

Figure. Intense 68Ga-FAPI uptake within cases of acute anterior (left) and posterior (right) myocardial infarction. Tracer uptake corresponds to the area of infarction detected on CMR assessment with late gadolinium enhancement.

Abstract number: O25

Synthetic workflow for validation of wall shear stress estimated using plane wave in carotid stenosis

Ke Yang[1,2], Peter Hoskins[2], Chunming Xia[1], George Corner[2], Zhihong Huang[2]

1. School of Mechanical and Power Engineering, East China University of Science and Technology
2. School of Science and Engineering, University of Dundee

Introduction: It is known that atherosclerosis progresses as an interplay between mechanical forces and biology. The wall shear stress (WSS) is the viscous drag of blood on the arterial wall. WSS may be estimated from the velocity gradient at the vessel wall. This presentation will investigate the measurement of WSS in a carotid stenosis model using plane wave imaging.

Methods: A synthetic approach was used in idealised straight tube stenoses using a combination of computational fluids dynamics (CFD) and acoustic simulation. Different stenosis models were made of 0, 20, 40, 60, 80% by diameter as a shape of cosine. All models were meshed, and a realistic carotid flow waveform was used as input. CFD was undertaken using Ansys; which provided the 3D 3-component time varying flow field. Ultrasound simulation was undertaken using Field II. The CFD data provides the ground-truth data that is also the trajectory of simulated scatterers. The vector flow imaging method based on plane wave (vector doppler and speckle tracking) was used to obtain the velocity field. This provides realistic ultrasound data from which the velocities and WSS were estimated and compared with the ground truth data obtained using CFD.

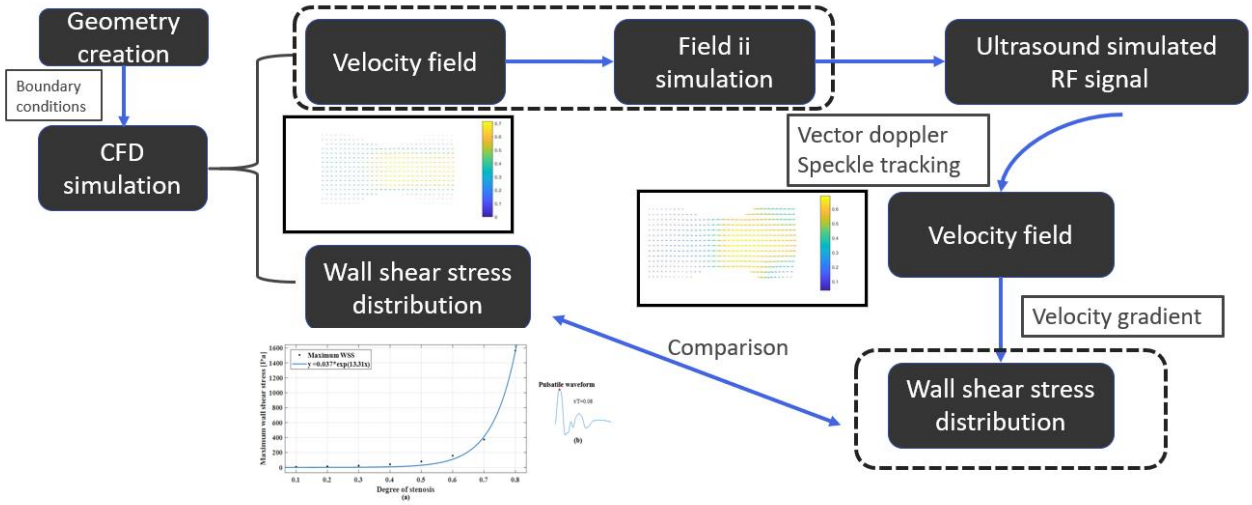

Fig. 1 The workflow of the measurement of Wall shear stress in the stenosis vessels.

Results: The CFD result shows the maximum WSS was found on the middle of stenotic region in all stenotic cases with a maximum value of 23.24 Pa in the 30% stenosis. The highest velocity in 30% stenosis which could be measured using plane wave is 0.69 m/s. The WSS obtained from ultrasound simulation showed good agreement with CFD.

Conclusions: Realistic flow fields could be simulated using the workflow allowing comparison between ground truth and measured WSS data. The workflow could be further developed to incorporate plaque with different acoustic properties.

Contact: 2397272@dundee.ac.uk

Abstract number: O26

Longitudinal TSPO PET imaging with [18F]LW223 in a rat myocardial infarction model

Mark G. MacAskill[1,2], Victoria Reid[1,2], Carlos J. Alcaide-Corral[1,2], Timaeus E. F. Morgan[1,2], Agne Knyzeliene[1,2], Catriona Wimberly[2], Lewis Williams[3], Nikki L. Sloan[3], Marc R. Dweck[1], Gillian A. Gray[1], David E. Newby[1], Christophe Lucatelli[2], Sally L. Pimlott[4,5], Andrew Sutherland[3], Adriana A.S. Tavares[1,2].

1. University/BHF Centre for Cardiovascular Science, University of Edinburgh, Edinburgh, UK.
2. Edinburgh Imaging, University of Edinburgh, Edinburgh, UK.
3. WestCHEM, School of Chemistry, University of Glasgow, UK.
4. School of Medicine, University of Glasgow, UK.
5. NHS Greater Glasgow and Clyde, UK.

Introduction: For several decades, the 18kDa Translocator protein (TSPO) has been a molecular imaging target for inflammation. We have developed a novel TSPO ligand, LW223, which has binding independent of the rs6971 polymorphism, good in vivo characteristics and is able to detect macrophage induced inflammation after myocardial infarction in a rat model (1). This study aims to map the temporal expression of TSPO within the heart following sham and myocardial infarction surgery in rats.

Methods: Adult male Sprague-Dawley rats underwent cardiac reperfusion injury (30 min) to induce MI. At 24 hours, cardiac troponin I was measured and [18F]LW223 PET/CT imaging was performed on days 2, 7, 14 and 28. Sham operated rats were used as controls. As demonstrated previously (1), [18F]LW223 transfer to myocardial tissue is highly dependent on perfusion changes and therefore SUV data was perfusion corrected using the de Grado model and PMOD software.

Results: A range of infarct sizes resulted from reperfusion injury, as evident in the troponin I measurements (6362±3197 ng/L, range 2583-10970). The highest [18F]LW223 binding was within the infarct in the apical-mid anterior wall of the MI group. This signal peaked at day 2 after infarction and a second phase of increase was detected on d28. There appear to be no major changes in the remote myocardium across all timepoints and groups.

Conclusion: This initial pilot analysis appears to suggest a two-phased TSPO response within the infarcted myocardium. Validation of the myocardial blood flow corrected SUV approach against our previously used method (BPTC) is now underway. The relation between [18F]LW223 binding and cardiac function (ultrasound) and detailed ex-vivo autoradiography and histology is also being carried out.

1.MacAskill et al. J. Nucl. Med. 2021;62:536–44.

Contact: mark.macaskill@ed.ac.uk

Poster Sessions

Abstract number: P1

Potential solution to stop the improper use of abdominal x-rays for abdominal pain

Winnie Tam

University of Leeds

Background: Abdomen x-rays (AXR) are a commonly requested radiographic examination for non-specific acute abdominal pain. However, recent evidence indicates that one in three patients are discharged from A&E without a diagnosis for their abdominal pain, questioning the role of abdomen x-ray in this clinical pathway.

Method: A literature review of studies and guidelines, dated from 1964 to 2018, was conducted, looking at AXR's effectiveness. The algorithm was constructed based on BMJ best practice guidelines and was coded with Python 3[1].

Result: Despite the documented ineffectiveness of AXR for supporting a definitive diagnosis or leading to a correct treatment alternation [2-14] and the advancement in CT and ultrasound, there was no dramatic decrease of the AXR used. Only 32% of AXR requests adhered to the Royal College of Radiologists guidelines [14-15], which may contribute to the high rate of further imaging and insignificant findings. Since abdominal pain is a symptom for all the justified and most of the unjustified indications, a way to help referrers to distinguish differential diagnoses is urgently required.

Conclusion: The conflicting evidence-base reflects the complexity of the use of AXR, and the issues around guidelines and departmental cultures. More research on this topic is required in the context of the resource usage and radiation risk involved in AXRs. An algorithm was constructed using BMJ Best Practice guidelines to assist referrals for acute abdominal pain [16-20]. However, this study suffered from a few limitations. The algorithm has not been used clinically; further testing is needed.

Contact: telex@wstam.uk

Abstract number: P2

Analysis of Positron Emission Tomography Data for Tumour Detection and Delineation

Wenhui Zhang[1], Surajit Ray[2]

Mathematics and Statistics, University of Glasgow

Recent developments in statistical image analysis and machine learning are culminating towards developing innovative tools for automatic analysis of three-dimensional radiological images — PET (Positron Emission Tomography) images. Statistical imaging together with other machine learning techniques are the epitome of digitalizing healthcare and offers many opportunities for providing patients with personalized medicine/therapy and reducing the cost of diagnosis/treatment. However, the three major challenges in radiology are: (1) increasing demand for medical imaging; (2) decreasing turnaround times caused by mass data; (3) diagnostic accuracy that should lead to a quantification of images. To address these challenges along with ethical issues regarding the use of Artificial Intelligence in patient care, there is a need to develop a new framework of statistical analysis which can be readily used by clinicians and can be trained with a relatively lower number of samples. In this project, we have developed a kernel-based method on PET image segmentation which will be more direct for tumour detection, delineation, monitoring and radiotherapy planning. We are currently working on combing other complementary information, such as CT(Computed tomography) images. The kernel-based method is a non-parametric regression technique which can corporate 3D information for a set of images. It is also computational efficient and can produce reproductive and robust results compared with other statistical methods. Another advantage of the kernel-based methods is that there is a great potential for developing a probabilistic approach with uncertainty measurement along with the segmentation.

Contact: w.zhang.2@research.gla.ac.uk

Abstract number: P3

Sex differences in the murine brain identified using [18F]LW223 PET, a marker of TSPO expression in vivo

Agne Knyzeliene[1,2], Mark G. MacAskill[1,2], Catriona Wimberley[2,3], Carlos J. Alcaide-Corral[1,2], Timaeus E. F. Morgan[1,2], Nikki Sloan[4], Christophe Lucatelli[2], Sally L. Pimlott[5], Andrew Sutherland[4], Adriana A. S. Tavares[1,2]

1. BHF-University of Edinburgh Centre for Cardiovascular Science, University of Edinburgh
2. Edinburgh Imaging, University of Edinburgh
3. Centre for Clinical Brain Sciences, University of Edinburgh
4. School of Chemistry, University of Glasgow
5. West of Scotland PET Centre, Greater Glasgow and Clyde NHS Trust

Introduction: The 18 kDa translocator protein (TSPO) is a well-known biomarker of neuroinflammation and also plays a role in a number of homeostatic functions, including steroidogenesis. Recently, clinical Positron Emission Tomography (PET) imaging studies with TSPO radiotracers have identified sex differences in TSPO expression in the adult human brain (Tuisku et al. 2019, PMID: 31363804). This study aimed to assess if TSPO expression in the adult mouse brain is also sex dependent. To address this aim we used our novel TSPO PET radiotracer [18F]LW223 (MacAskill et al. 2020, PMID: 32859708).

Methods: Nine male and five female C57Bl6/J mice (13.6±5.4 weeks, 26.8±5.4 g, mean±SD) underwent PET scanning over 2 hours following administration of [18F]LW223 (i.v. tail vein, 6.7±3.6 MBq). Whole body and regional brain analyses were performed by drawing volumes of interest (VOI) around different target regions and the average standard uptake values (SUVs) between 90-120 minutes were calculated. Statistical differences were assessed using two-way ANOVA with Sidak's post hoc test (alpha = 0.05).

Results: Male and female mice showed similar uptake of [18F]LW223 across the peripheral organs included in the analysis (i.e. heart, lungs, adrenals, kidneys and spleen). No statistical differences were detected at the whole-body level. However, regional analysis of radiotracer binding in the brain showed that female mice had lower [18F]LW223 uptake across all regions of the brain, with significant differences in the hypothalamus, olfactory bulb, amygdala, brain stem, basal forebrain septum and midbrain.

Conclusions: Data suggest that TSPO may play a role in endocrine control and reproduction, given the largest difference between groups was measured in the hypothalamus – a key brain region involved in controlling these functions (Clasadonte et al. 2018, PMID: 29076504; Tena-Sempere 2017, PMID: 28059155). This study highlights the need to conduct sex-controlled comparisons when assessing TSPO expression in the murine brain.

Contact: a.stadulyte@sms.ed.ac.uk

Abstract number: P4

Brain Networks: Challenges of high correlations and how to overcome them

Philipp Loske[1], Björn O. Schelter[2,3]

1. Aberdeen Biomedical Imaging Centre, University of Aberdeen
2. TauRx Therapeutics Ltd., Aberdeen
3. Institute for Complex Systems and Mathematical Biology, University of Aberdeen

Brain connectivity networks are representations of the brain as a complex interacting system. They are constructed based on measurements extracted from various imaging modalities. These measurements are often linked using the correlation coefficient. This can be the correlation of time series measuring brain activity recorded in functional MRI or the correlation of morphological features extracted from structural MRIs. Correlation networks have proven valuable for the understanding of brain development, function and ageing up to providing insights to the early-onset and progression of neurological diseases.

While brain correlation networks provide an objective and informative non-invasive tool to study the brain, the direct analysis of the correlation coefficient can be misleading. The correlation coefficient does not differentiate between direct and indirect links, which can lead to drawing false conclusions about the network. Separating direct from indirect links is a challenging task. If the network contains highly correlated nodes which is often the case in brain networks, existing methods fail to correctly reconstruct the actual networks.

Here, we present a novel method that separates direct from indirect links in networks containing highly correlated nodes. We conduct a simulation study to compare the method to existing methods and show that the method correctly reconstructs the actual underlying topology where existing methods fail.

Applying this method to brain connectivity networks can help to avoid making erroneous conclusions about network structures. It enables robust filtering of indirect links in the presence of high correlations, which was previously not possible. This can help in improving the understanding of the brain as an interacting system and increase the interpretability of brain networks for medical applications.

Acknowledgements: PL acknowledges financial support from Medical Research Scotland (Grant No: RG14565).

Contact: p.loske.18@abdn.ac.uk

Abstract number: P5

Pre-operative Coronary Artery Calcification (CAC) in patients undergoing potentially curative colorectal cancer surgery

Shea Roddy[1], Christopher J Payne[2], Mansoor Husain[2], Carol E Gray[3], Prasad Guntur[1]

1. Department of Radiology, Ninewells Hospital, Dundee
2. Department of Colorectal surgery, Ninewells Hospital, Dundee
3. Department of Anaesthesia, Ninewells Hospital, Dundee

Aims: Pre-operative assessment aims to optimise know medical co-morbidities and stratify risk of adverse outcomes following surgery. Coronary Artery Calcification (CAC) has been shown in non-surgical populations to predict future cardiac events and long-term survival. We aimed to investigate a correlation between CAC, using the Ordinal CAC score on pre-operative computed tomography (CT) scan, and recognised risk factors for heart disease (HD).

Methods: Fifty consecutive patients undergoing colorectal cancer surgery in 2017/18 were identified from a prospectively collected database. Records from the Pre-operative Assessment Clinic were reviewed for risk factors. Staging CT scans were reviewed by 2 observers, blinded to clinical variables. Patients were categorised to no CAC or mild CAC and severe CAC.

Results: Twenty-two (46%) patient had no or mild CAC and 54% had severe CAC. Male patients had a higher rate of severe CAC compared with female patients (66% vs. 18%), $p<0.005$. Patents aged ≥70 years had a higher rate of severe CAC (70%) compared with patients aged <70 years (35%), $p=0.014$. A history of heart disease was noted in 8 (16%) patients. 29% of patients with severe CAC had a history of HD, compared with no patients in the no or mild CAC group ($p=0.006$). 20 (71%) patients with severe CAC had no documented cardiac history.

Conclusions: The incidence of pre-operative CAC is high. In particular, a high proportion of patient with severe CAC had no documented HD. Identifying CAC in asymptomatic patient may represent an opportunity for additional risk factor modification and requires further attention with prospective observational trials.

Contact: shea.roddy@nhs.scot

Abstract number: P6

Are Reported Volume Abnormalities in Autism Consistent? A Meta-Analysis of Morphometric Data

Ms Michelle Sader[1], Dr Justin Williams[1], Dr Gordon Waiter[1]

1. Aberdeen Biomedical Imaging Centre, University of Aberdeen

Autism Spectrum Disorder (ASD) is a neurodevelopmental disorder characterised by difficulties in communication and behaviour. A variety of neuroimaging studies over the years exhibit structural abnormalities in those with ASD, yet there is no ubiquitously stated region of the brain associated with ASD. Authors note largely discrepant findings regarding affected region as well as age/sex associations with volume. Distinctly affected brain regions in ASD as well as inconsistencies in age/sex associations calls for a quantitative review of neuroimaging literature to identify and elaborate upon regions of the brain most pertinently associated with ASD. We performed a systematic review of ASD MRI literature as well as analysis of 40 individuals from the ABIDE II dataset. 47 publications were collected examining neuroanatomical structure in ASD relative to healthy controls (HCs). Contrary to an abundance of literature, no significant clusters differentiating brain volume between ASD and HCs were identified in both the collated dataset or age subgroups (0-21, 21+). Findings from analysis of the ABIDE II dataset corroborate meta-analytic results. We identified no significant difference in grey matter, white matter, subcortical and cerebellar volumes between those with ASD and HCs. Moreso, no significant associations between age and volume were identified. Negative neuroimaging findings suggest the neuroanatomy of ASD is inconsistent, and structural abnormalities are too diverse to pinpoint regions characteristic of ASD.

Acknowledgements: I would like to express my thanks and gratitude to my two supervisors, Dr Justin Williams and Dr Gordon Waiter. They have made this research possible with their essential advice and technical knowledge. I would also like to extend my sincere gratitude to the Northwood Charitable Trust for funding my PhD studentship.

Contact: r05ms19@abdn.ac.uk

Abstract number: P7

A Meta-Analytic Investigation of Grey Matter changes in Anorexia Nervosa

Ms Michelle Sader[1], Dr Justin Williams[1], Dr Gordon Waiter[1]

1. Aberdeen Biomedical Imaging Centre, University of Aberdeen

Recent research has shown Anorexia Nervosa (AN) to be highly dependent upon neurobiological function. One source of evidence has come from magnetic resonance imaging (MRI) using voxel based morphometry (VBM). Individual studies tend to be relatively small and no recent quantitative review has been published. We performed a systematic review of MRI coordinate literature to determine whether there were consistent changes in grey matter across studies. Utilising 24 publications with 1,183 subjects, meta-analysis revealed increased volume within the orbitofrontal gyrus and medial temporal lobe, and decreased volume in the rostral cingulate gyrus and superior/inferior parietal lobes. Separating data based on age revealed clusters in the adult-only literature within the genu of the anterior cingulate cortex (ACC). This is the first quantitative meta-analysis to date identifying increased brain structure in AN. Findings support recent neuropsychological studies identifying changes in episodic memory and may also suggest correlates of learned aversion to food.

Acknowledgements: I would like to thank and express my gratitude towards my two supervisors, Dr Justin Williams and Dr Gordon Waiter, as well as to the Northwood Charitable Trust for funding my PhD Studentship.

Contact: r05ms19@abdn.ac.uk

Abstract number: P8

The Cerebellum Plays More Than One Role in Appetite Control: Evidence from Typical and Pathological Populations

Ms Michelle Sader[1], Dr Justin Williams[1], Dr Gordon Waiter[1]

1. Aberdeen Biomedical Imaging Centre, University of Aberdeen

Dysregulated appetite control is characteristic of anorexia nervosa (AN) and obesity (OB), and is a subject of major public health concern. Whole-brain neuroimaging analyses and genetic evidence suggests the cerebellum plays a role in homeostatic and appetite control. This brain region is also implicated in both AN and OB with reports of aberrant volume compared to non-clinical populations. Significant genetic correlations and reduction in grey matter volume (GMV) across AN and OB prompts a large-scale investigation of cerebellar volume across weight and dysfunction of appetite regulation. We reviewed MRI literature to determine if there were consistencies in cerebellar GMV changes across studies for AN and OB. 20 publications were identified as either case-control studies (n=619) or regressed weight from normative data against brain volume (n=3,518). AN and OB analyses both showed consistently decreased GMV within the left cerebellum, but volume reduction was anterior for AN and posterior for OB, with minimal overlap. The normative analysis identified a cluster in the right posterior lobe. Findings suggest that more than one area of the cerebellum is involved in control of eating behavior and is differently affected in normal variation or pathological conditions.

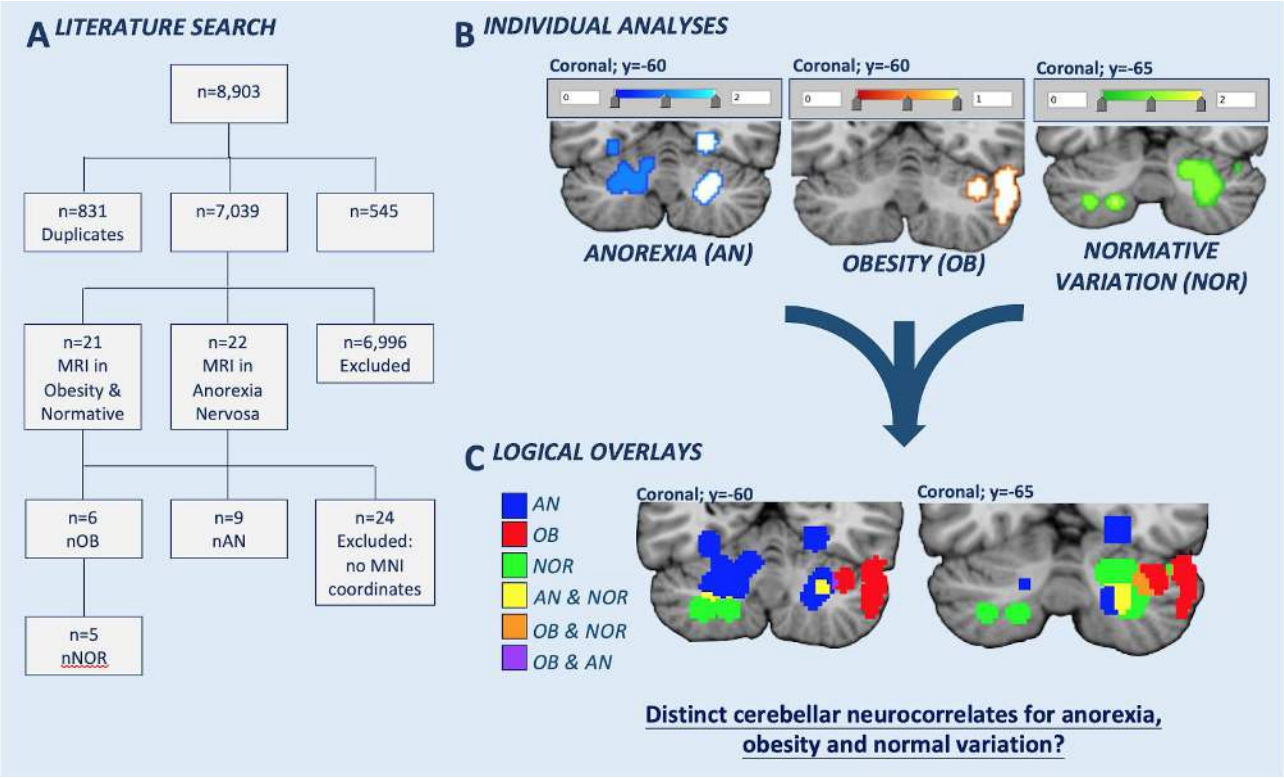

Acknowledgements: I would like to express my gratitude to my two supervisors, Dr Justin Williams and Dr Gordon Waiter for making this research possible. I would also like to extend my thanks to the Northwood Charitable Trust for funding my PhD studentship.

Contact: r05ms19@abdn.ac.uk

Abstract number: P9

Comparing Specific Absorption Rate (Tissue Heating) Management Methods for Parallel Transmit MRI at 7 Tesla

Sydney N. Williams[1], Jürgen Herrler[2], Patrick Liebig[3], Paul McElhinney[1], Sarah Allwood-Spiers[4], John E. Foster[4], Shajan Gunamony[1,5], Armin M. Nagel[6], David A. Porter[1]

1. Imaging Centre of Excellence, University of Glasgow, Glasgow, United Kingdom
2. Department of Neuroradiology, University Hospital Erlangen, Erlangen, Germany
3. Siemens Healthineers, Erlangen, Germany
4. NHS Greater Glasgow & Clyde, Glasgow, United Kingdom
5. MR CoilTech Limited, Glasgow, United Kingdom
6. Institute of Radiology, University Hospital Erlangen, Erlangen, Germany

Parallel transmit (pTx) can reduce RF field inhomogeneity present at 7T, but needs additional consideration for the specific absorption rate (SAR) and subsequent tissue heating due to the superimposed electromagnetic fields. Virtual observation points (VOPs) provide a common method for evaluating SAR in parallel transmit (pTx) MRI. The VOP approach uses an Eigenvalue clustering method to group voxels in electromagnetic field (EMF) simulations of realistic human body models. The clustering amount is set by an overestimation factor with respect to the "worst case" SAR configuration of complex pTx channels. It has been suggested to include as many EMF body model simulations at as many positions as computationally feasible in the VOPs to account for potential local SAR hotpots. Nevertheless, commercial pTx coils for 7T are typically supplied without the EMF-based VOPs and instead apply a constant safety factor for local SAR supervision, which can be overly conservative. In this abstract we compare the use of EMF-based VOPs in a self-built pTx head coil to constant safety factor VOPs in a commercial pTx coil of similar design. We investigate the local SAR values with 7T MRI scans in healthy volunteers. Comparing the VOPs' simulated and experimental performance in both coils, the commercial coil VOPs provide SAR estimates that are highly conservative compared to estimates from VOPs based on anatomical models, yet the image quality from both coils remains very similar (Figure 1). The self-built coil's EMF-based VOPs are closer to the modeled SAR deposition without clustering (Figure 2), thus allowing scanning within the IEC normal mode head limit of 10 W/kg, which wasn't feasible with the commercial coil. In the future, larger scale EMF simulations are required to explore the effect of subject anatomy and to optimize the use of VOPs for wider application.

Acknowledgements: We would like to acknowledge Tracey Hopkins, Rosemary Woodward, and Natasha Fullerton from the NHS Greater Glasgow & Clyde. We also thank Rene Gumbrecht and Robin Heidemann from Siemens Healthineers, Erlangen, Germany.

Contact: sydney.williams@glasgow.ac.uk

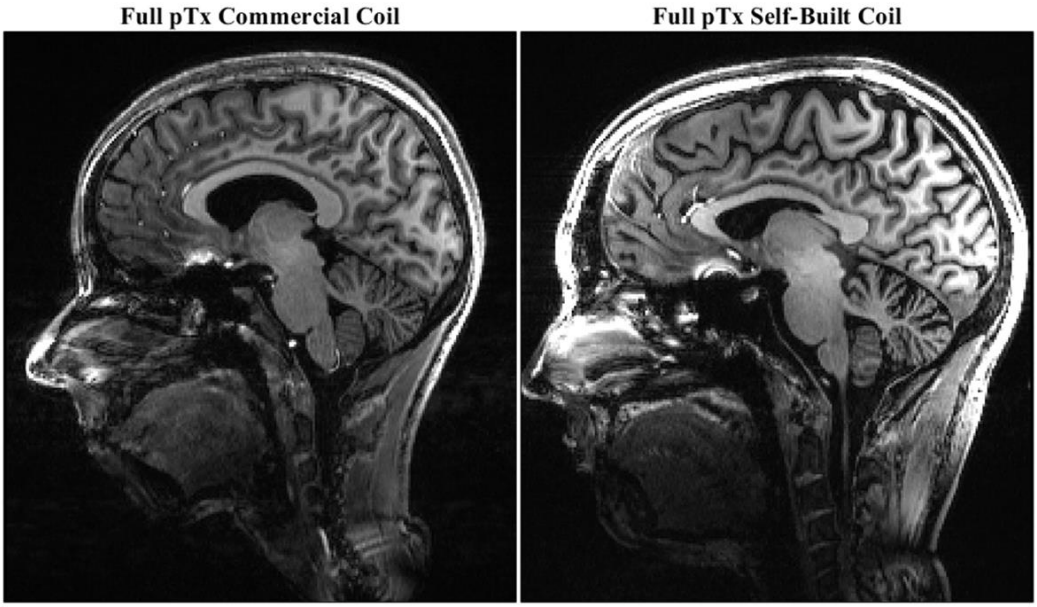

MPRAGE Sequence	Calc. SAR	Scanner Pred. SAR	Scanner Meas. 10 sec SAR	Scanner Meas. 6 min SAR
Commercial Coil: FOCUS Inv. + UP Exc.	11.68	11.87	10.65	10.30
Self-Built Coil: FOCUS Inv. + UP Exc.	3.02	3.08	2.53	2.71

Figure 1. Comparison of T1w MPRAGE images using all pTx pulses with the commercial coil (left) and self-built coil (right) for different subjects at different scanners. Both images were acquired with pTx inversion and excitation pulses designed for their respective coils and are windowed the same. The table lists calculated, scanner-predicted, and scanner-measured local SAR in W/kg. The image quality is comparable, but the estimated SAR is lower with the self-built coil and EMF-based VOPs.

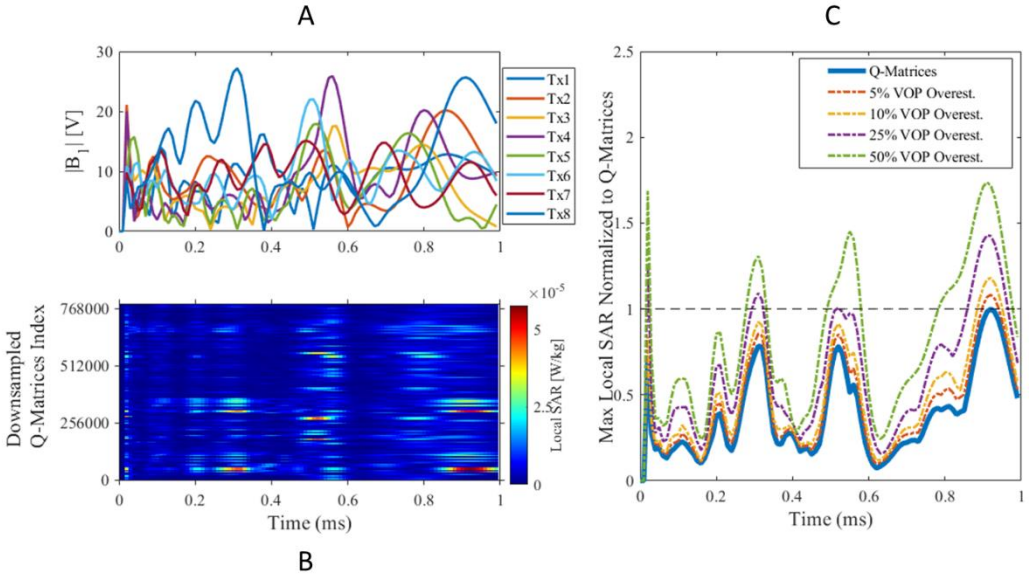

Figure 2. Local SAR for a 5° pTx excitation pulse. A) Pulse magnitude waveform for 8Tx channels; B) Instantaneous SAR for the pulse in MPRAGE using downsampled, uncompressed Q-matrices from the EMF simulation; C) Max local SAR for each time point of the pulse for the full Q-matrices and VOPs with 5%, 10%, 25%, and 50% overestimation, all normalized to the maximum of the Q-matrices' SAR. Different time points of the pTx pulse (i.e., different amplitude and phase configurations) lead to varying levels of VOP overestimation relative to the Q-matrices, but importantly the VOP-derived estimate is always overestimated.

Abstract number: P10

Drug discovery and repurposing using biomimetic chromatography and body-on-chip technology

Liam Carr[1,2], Mark G. MacAskill[1,2], Patrick W. F. Hadoke[1], Adriana A. S. Tavares[1,2]

1. BHF-University of Edinburgh Centre for Cardiovascular Science, University of Edinburgh, UK.
2. Edinburgh Imaging, University of Edinburgh

The drug discovery pipeline is lengthy and expensive with high rates of attrition. On average, it takes 12 years and a $1.3bn investment for a drug to reach the market, largely inflated by the time and money invested into failed candidates. Only approximately 25% of small molecule drug candidates from pre-clinical studies progress to phase 1 clinical trials, at which point new drugs have a likelihood of approval of roughly 7.6%, indicating a need for more efficient lead compound selection and better predictors of in vivo success in humans during early drug discovery. We aim to combine the use of biomimetic chromatography and body-on-chip technology, validated using pre-existing in human in vivo data from positron emission tomography (PET) radiotracers, to accurately predict the in vivo success of a drug in human clinical trials at an early stage of drug discovery. Immobilised artificial membrane, human serum albumin (HSA) and C18 chromatography will be used for 7 compounds, previously used as radiotracers in humans. We hypothesise that data from biomimetic chromatography can be used to accurately predict plasma protein binding (PPB) and blood-brain-barrier penetration of the 7 compounds compared to in-house ultrafiltration data and the %injected dose values from pre-existing in vivo human PET data, respectively. Data from biomimetic chromatography will then be integrated into a novel kinetic model, along with body-on-chip derived biodistribution data, to predict human in vivo success. If successful, this will aid in the selection of lead compounds and potentially increase the translational capacity of drug candidates from pre-clinical to clinical settings. Preliminary HSA chromatography experiments using the chemotherapeutic docetaxel and the GABAA antagonist flumazenil gave predicted PPB values of 80.8% and 39.6% respectively, compared to reported literature PPB values of 93% and 40% respectively, indicating potential for accurate prediction of PPB upon further validation with more compounds.

Acknowledgements: LC is funded by a NC3R/Unilever studentship (NC/V001302/1).

Contact: Liam.Carr@ed.ac.uk

Abstract number: P11

Machine Learning methods for the classification of Dementia using images from the Genetics of Diabetes Audit and Research in Tayside Scotland (GoDARTS) cohort

Esma Mansouri-Benssassi[1], J Douglas Steele[1], Alexander S F Doney[1], Susan Krueger[1], Emily Jefferson[1]

1. University of Dundee

Background: Early detection of dementia can be particularly useful in the development of preventive measures affecting the progress of the disease. In this work we present preliminary results in applying machine learning techniques to routinely acquired medical images.

Materials and Methods: Patients with dementia diagnosis within 2 years of their scans are compared with a control group without evidence of dementia diagnosis or a follow up for over 5 years. 24 cases (Dementia) and 24 controls (no Dementia) are matched by sex and age with 19 males and 5 females with an average age of 76. Within the cases group 14 are diagnosed with Alzheimer dementia, 9 with Vascular Dementia and 1 with a non-identified type. Pre-processing steps based on Voxel-Based Morphometry analysis are applied on T1-weighted images where we apply normalisation, segmentation, and smoothing techniques. We apply a feature selection process where cases and controls are statistically compared. This method reduces the number of features by identifying voxels with significant difference. Two Support Vector Machine (SVM) models with Radial basis function (RBF) kernels are trained separately for White Matter (WM) and Grey Matter (GM) tissues. The training and features selection is applied in a nested cross-validation with 5-folds.

Results: The GM SVM shows an overall accuracy of 85.7% with a sensitivity of 0.81 and Specificity of 0.90. The WM overall accuracy is 76.47 % with a sensitivity of 0.88 and specificity of 0.62.

Future work: Preliminary results demonstrate the efficacy of the pipeline in reaching high accuracy using small heterogenous routinely acquired data where results are comparable to models trained on research grade data. Future work will include creating ensemble algorithms with multimodal data by introducing other factors such as genetic and clinical data.

Acknowledgements: This work is part of the Prediction of Individual Patient Risk of Dementia (PIPaRD) project, which is one of two medical exemplar projects enabled through the 5-year PICTURES programme (InterdisciPlInary Collaboration for efficient and effective Use of clinical images in big data health care RESearch), funded by the Medical Research Council (MRC) with additional support from the Engineering and Physical Sciences Research Council (EPSRC) as part of Health Data Research UK (HDR UK).

https://www.imageonamission.ac.uk/

Contact: emansouribenssass001@dundee.ac.uk

Abstract number: P13

Providing a neuro-imaging evidence-base for motor neuro-rehabilitation

Magda Mustile[1], Dimitrios Kourtis[1], Martin G. Edwards[2], David I. Donaldson[3], Magdalena Ietswaart[1]

1. Psychology, Faculty of Natural Sciences, University of Stirling
2. Institute of Research in the Psychological Sciences, Université catholique de Louvain, Belgium
3. School of Psychology and Neuroscience, University of St Andrews

A major limitation of neuro-rehabilitation of motor disorders is the lack of a true neuroimaging evidence-base. The neural correlates of movement are largely unknown because movement is mostly restricted in neuroimaging contexts. At Stirling we have developed the Mobile Cognition approach, examining brain activation in motion. We can now investigate brain processes during walking through the use of mobile EEG. This is furthermore a multi-modal approach, where brain signals and non-brain signals (such as gait) are measured concurrently. Motor imagery and action observation are accepted rehabilitation techniques in the recovery of movement of lower limb deficits, mainly following stroke. However, there is a lack of evidence on how these techniques are of benefit by activating the cortical motor processes involved in walking, as assumed following a Hebbian learning rationale (firing is rewiring). Here we present the evidence for the extent to which cortical motor processes are activated by motor imagery of walking and action observation of walking, compared to actual motor execution of walking. We find that motor imagery of walking does indeed show functional equivalence with actual execution, which would mean that motor areas of the brain can be 'jogged' through imagery of walking. However, brain activity of action observation of walking does not resemble actual execution. This is significant, because if action observation in itself does not activate cortical motor processes, as is generally assumed, then the utility of action observation in motor rehabilitation practice is questionable.

Contact: magda.mustile@stir.ac.uk

Abstract number: P14

3D-printed tissue-mimicking and cell compatible hybrid hydrogels for ultrasound and microbubble-mediated drug delivery research

Lauren Gilmour[1], Roger Domingo-Roca[1], Craig Bradley[1], Joseph C Jackson[2], Richard O'Leary[2], Mairi Sandison[1], Helen Mulvana[1]

1. Department of Biomedical Engineering, University of Strathclyde
2. Department of Electronic and Electrical Engineering, University of Strathclyde

Microbubbles administered intravenously to circulate systemically can be driven using ultrasound for contrast-enhanced imaging and drug delivery. Despite promising results in vitro and in vivo, the mechanisms involved remain incompletely understood, hindering optimisation and eventual clinical translation. Mechanistic insight is impossible in vivo, while in vitro studies often lack many important physiological parameters, limiting their utility. Tissue-mimicking hydrogels adapted for light-based 3D-printing can be used to develop microvessels to reproduce physiologically relevant features, smaller than 50 microns. Biocompatible hydrogels that support cell adhesion and growth are an area of interest across several fields, and could provide a more relevant in vitro model of ultrasound, microbubble, cell and tissue interactions.

The aim of this work is to determine what are the best hydrogel compositions that offer both tissue-mimicking acoustic and mechanical properties, and cell compatibility and adhesion. To approach this, photo-responsive hybrid hydrogels were prepared using previously characterised tissue-mimicking BEMA 20wt% hydrogel and cell adhesion promoting polymers including PVA, acrylic acid and GelMA along with photoinitiator (LAP) and photoblocker (tartrazine). Test samples of the hydrogels were added to 8-well plates and cured in a UV chamber. After solidification, the samples were sterilised and incubated in serum free media for 1 hour. Smooth muscle cells were cultured in 1:1 Waymouth's:Ham's F12 media containing 10% fetal bovine serum with 1% penicillin-streptomycin and 1% L-glutamine at 37o Cin 5% CO2 and 80% humidity. Dead/live assays were performed using propidium iodide (PI) and Calcein AM, and assessed by fluorescence microscopy. We show that photo-responsive, tissue-mimicking hydrogels can be cell-compatible, potentially offering a suitable platform for ultrasound-microbubble experiments. Once cell compatibility is established, materials will be optimised for 3D-printing with the aim of producing high resolution, physiologically relevant geometries for controlled investigation of microbubbles for the application of targeted drug delivery.

Contact: lauren.gilmour@strath.ac.uk

Abstract number: P15

Low Cost Photoacoustic Computed Tomography System Based on Adaptive Back Projection Reconstruction

Yang Zhang[1], Shufan Yang[2,3], Jichuan Xiong[1], Xuefeng Liu[1]

1. School of Electronic and Optical Engineering, Nanjing University of Science and Technology
2. Centre for Medical and Industrial Ultrasonics, University of Glasgow
3. School of Computing, Edinburgh Napier University

Photoacoustic Computed tomography (PACT) is a novel technique of noninvasive medical imaging based on the photoacoustic effect [1]. Photoacoustic technology has the advantage of excellent contrast agents and molecular targeting at imaging depth [2]. Current PACT research mainly focuses on the optimizing of the system components such as the laser source and the probe, with expensive multi-array ultrasound transducers and data acquisition units. The high cost of those equipment prevents the widespread adoption into research communities and potential clinic applications. However, the reconstructed images have few unwanted artifacts, which affects fidelity of reconstructed images [3]. Since the conventional back-project image reconstruction algorithm is assumed on ideal experiment conditions. Those constraints are not possible to achieve when using low-cost equipment, especially with single transducers setup.

We proposed to use a single ultrasound transducer to rotate around our tissue-mimicking phantom with human hair. In this paper, we proposed an adaptive back projection reconstruction method to improve the quality of reconstructed photoacoustic images by eliminating the unwanted artifacts using an adaptive method. Firstly, the appropriate threshold is selected according to the frequency of the photoacoustic signal. Then, the intensity of the photoacoustic signal is adjusted adaptively according to the threshold. Finally, the back projection algorithm is used to reconstruct the photoacoustic image.

The proposed method was used to conduct photoacoustic tomography experiments on tissue-mimicking phantoms buried with human hair. Experiments show that this method can effectively eliminate the image artifacts with the conventional back-projection algorithm after our adaptive adjustment, and the peak signal-to-noise ratio of the reconstructed image is increased by 12%. The low-cost PACT system with single transducer reduces the estimated 80% cost of the overall system compared with equivalent platforms.

Contact: 218104010144@njust.edu.cn; s.yang@napier.ac.uk

Abstract number: P16

Assessment of Lungman Anthropomorphic Phantom

Amy Oana[1], Mark Worrall[1]

1. Medical Physics, Ninewells Hospital, Dundee

The Lungman anthropomorphic phantom was acquired for use in optimisation studies within NHS Tayside. To determine whether this phantom is representative of the local patient cohort, a comparison was carried out using standard exposure protocols by means of patient dose audits. The perspex equivalent thickness was also estimated to compare with similar studies.

A patient dose comparison was carried out for chest posterior-anterior examinations by carrying out a dose audit from 1st September 2019 to 11th March 2020 for a computed radiography (CR) room without using an anti-scatter grid, and a digital radiography (DR) room using an anti-scatter grid. Lungman was exposed using local room protocols for each of these rooms, with the kerma area product (KAP) and exposure parameters (kVp and mAs) compared to those of the patient cohort from the dose audit.

The perspex equivalent thickness was estimated by varying perspex thickness and recording the sensitivity value (S-value) to compare with the S-value of an exposure of Lungman using the same exposure conditions. The perspex thickness plotted against the S-value was fitted to an exponential trendline. The Lungman exposure had an S-value of 373, giving a perspex equivalent thickness of 11.4cm. This was comparable to results determined using a similar method in the literature.

The patient dose comparison indicated that the KAP delivered to Lungman for both techniques fell within the distribution of KAP delivered to patients, slightly below the mean KAP. The kVp and mAs used for each technique were also slightly lower than the mean kVp and mAs used for the patient cohort but were within the distributions for each. This is indicative that Lungman represents a slimmer member of our patient cohort.

Acknowledgements: Thank you to our radiographer colleagues for assisting us with phantom positioning to allow for best comparison with our patient cohort.

Contact: amy.oana@nhs.scot

Abstract number: P17

Developing new biomarkers for imaging oligodendrocyte function in vivo

Robert C. Shaw[1,2], Timaeus E. F. Morgan[2,3], Sally L. Pimlott[4], Christophe Lucatelli[2], Andrew Sutherland[3], Adriana Alexandre S. Tavares[1,2]

1. University/BHF Centre for Cardiovascular Sciences, University of Edinburgh, UK
2. Edinburgh Imaging, University of Edinburgh, UK
3. School of Chemistry, University of Glasgow, UK
4. NHS Greater Glasgow and Clyde, UK

Introduction: Myelin, produced by oligodendrocytes, breaks down in multiple sclerosis; leading to loss of function, degeneration and disability. Currently, there is no cure or way to image oligodendrocytes activity in vivo. This project aims to develop new imaging biomarkers to assess oligodendrocyte function in vivo, by targeting the sphingosine-1-phosphate-5 (S1P5) receptor as a potential marker of oligodendrocyte function in vivo positron emission tomography (PET).

Methods: Rat brain tissue from adult rats (10 weeks, 370±4.08 g, n=3) was used. Immunofluorescence stains conducted were S1P5, Olig2, CC1, NG2, Sox6 for oligodendrocytes across developmental stages as well as GFAP, Iba1 and NeuN for astrocytes, microglia, and neurons respectively. A selective S1P5 agonist, TEFM180 was labelled with tritium and used to conduct receptor ligand binding assays and autoradiography experiments on naïve rat brain tissue.

Results: S1P5 co-localised with most CC1 and Olig2 positive cells, while NG2 showed co-localisation with S1P5 only in some cells. Sox6 co-localised with certain S1P5-positive cells. GFAP and Iba1 did not co-localise with S1P5 and the cells were morphologically distinct. There appeared to be some co-localization with NeuN. Receptor ligand binding assays showed that non-specific binding rose at increasing [3H]TEFM180 concentrations (Fig.1A) and high concentrations of rat brain protein were required to obtain a low degree of specific binding (Fig.1B). Altering the incubation temperature or buffer had no significant effect, however increasing time appeared to reduce non-specific binding. Higher specific binding was measured using autoradiography techniques (37.62-70.96%) (Fig.1C and 1D).

Discussion: Our immunofluorescence results confirm that S1P5 is a valuable target to investigate oligodendrocyte function, being selectively expressed on glia cells, specifically mature oligodendrocytes. The selective S1P5 agonist, TEFM180, is a non-specific ligand with low specific target engagement. Given the promising role of S1P5 in oligodendrocyte biology, new compounds with improved binding kinetics are needed for development as imaging biomarkers.

Contact: s1842712@ed.ac.uk

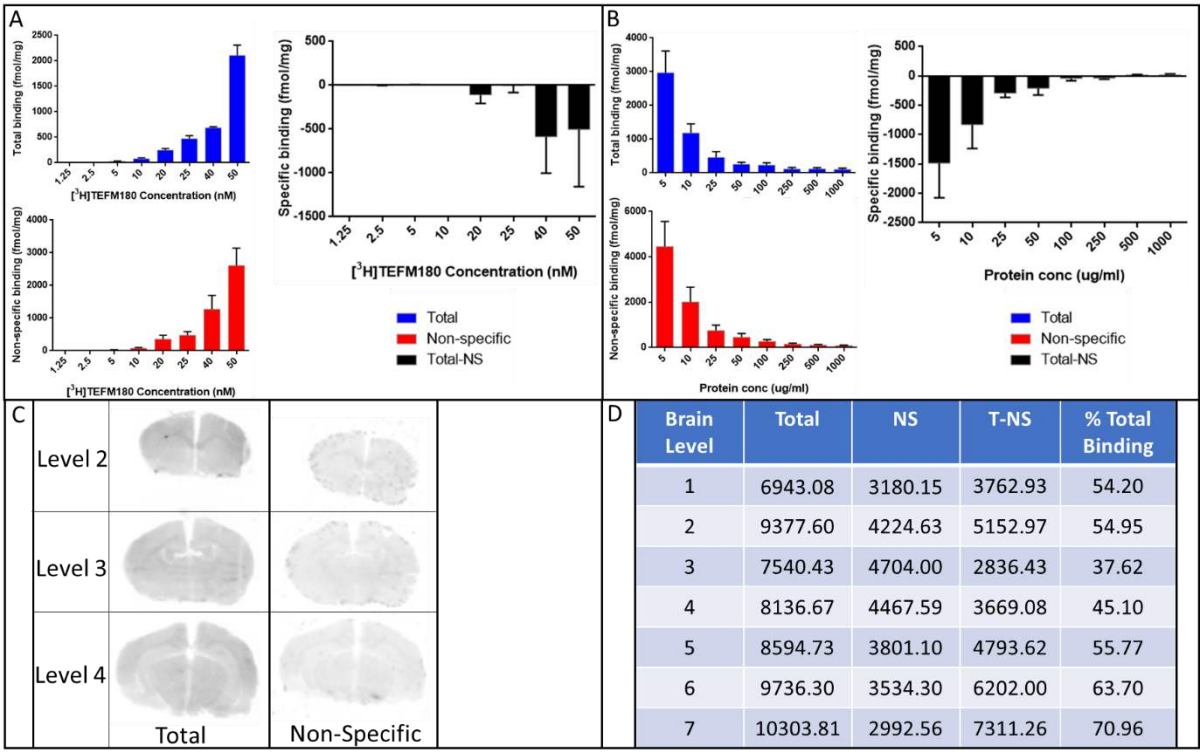

Brain Level	Total	NS	T-NS	% Total Binding
1	6943.08	3180.15	3762.93	54.20
2	9377.60	4224.63	5152.97	54.95
3	7540.43	4704.00	2836.43	37.62
4	8136.67	4467.59	3669.08	45.10
5	8594.73	3801.10	4793.62	55.77
6	9736.30	3534.30	6202.00	63.70
7	10303.81	2992.56	7311.26	70.96

Figure 1: Key binding assay and autoradiography results. (A) [3H]TEFM180 concentration assay showing increasing non-specific binding at high concentrations of [3H]TEFM180, indicating non-saturable off target binding. (B) Protein concentration assay, high levels of protein are required to reduce non-specific binding, indicating low target expression in whole rat brain homogenate (C) Representative images of [3H]TEFM180 autoradiography. (D) Values gained for [3H]TEFM180 autoradiography demonstrating a saturable binding (37.62-70.96%).

Abstract number: P18

Study to establish the parameter space of ultrasound imaging based detection of tissue stiffness variations

Patricia Foia[1], Dominik Duklas[1], Mark Hodnett[2], Anthony Gachagan[3], Laura Machesky[4], Helen Mulvana[1]

1. Department of Biomedical Engineering, University of Strathclyde,
2. National Physical Laboratory
3. Centre for Ultrasonic Engineering, Department of Electrical and Electronic Engineering, University of Strathclyde
4. CRUK The Beatson Institute, University of Glasgow

Pancreatic cancer is a devastating disease with an 8% 5-year survivability [1] if detected while it's still localised. The lack of symptoms in the early stages means that half of diagnoses are made after the cancer has metastasized. Due to the anatomical positioning of the pancreas and the lack of symptoms, clinicians use CT scans for detection. Here we focus on ultrasound imaging, as it is a cheaper and less difficult examination to perform, though, it cannot image the pancreas to the same resolution as other imaging techniques. However, it is ideally suited to detecting alterations in stiffness. We can use tissue stiffness as a biomarker for disease, due to the variation in healthy and diseased tissue. Here we assess, through computational and experimental methods, the parameter space for the detection of such variations in B-mode.

In OnScale, we computationally model a sample of diseased tissue surrounded by healthy tissue, in order to mimic early disease stage. A single array transducer is placed at a varying distance from the tissue, which has a varying stiffness and is driven with a range of frequencies (1-30 MHz, in steps of 5 MHz). The amplitude of the reflected signal at each tissue boundary is recorded to establish the lowest driving frequency that allows inclusion detection. This can be used to identify a given dimension inclusion, and the smallest stiffness difference that can be detected. To validate our simulation we set up a 3.5 MHz transducer with a focus at 70 mm and a PVA-based tissue mimicking phantom of various stiffness difference in a bath of degassed water and use the previously mentioned methodology.

The work undertaken aims to establish the parameter space of B-mode imaging as a tissue stiffness detection protocol.

[1] R. L. Siegel et al., CA Cancer J Clin, 68(1):7-30, 2018.

Acknowledgements: Medical Research Scotland (funder)

Contact: patricia.foia@strath.ac.uk

Abstract number: P19

Association of the regional cortical complexity with fluid cognition and life course factors

Nafeesa Nazlee[1], Dr Gordon D Waiter[1], Dr Anca Sandu-Giuraniuc[1]

1. Aberdeen Biomedical Imaging Centre, University of Aberdeen, Scotland, UK

Fractal dimension (FD) analysis provides a quantitative description of the brain's structural complexity. Brain complexity and cognitive abilities are positively associated and decrease with advancing age. The age-related decrease in structural complexity and cognition may arise from many sources including biological and environmental factors. We investigated a single sample of 5607 middle to older aged adults (2848 females, age range 45-79 years) regarding the association of the modifiable life course factors (years of education, BMI, income, alcohol use, smoking status, and moderate physical activity) with the regional cortical ribbon complexity (FD) and fluid intelligence (FI) score. The data was obtained from the UK Biobank imaging cohort and the participants had no known neuropsychological disorder. The association between the FI score and FD was significant in all regions with dominance in the right hemisphere and right temporal lobe. Multiple regression models were carried out with the adjustment of age, sex and we found that BMI has a significant negative association with the left hemisphere and left parietal lobe complexity; significant positive association of moderate physical activity of 4 days/week with left frontal lobe complexity whereas income (> £31000/annum) has a positive association with several brain region's complexities. Further adjustment for these life course factors revealed that the association between FI and FD was significant in the left and right hemisphere, and frontal, temporal and parietal lobes with exception of the occipital lobe. To identify the possible mediators that might affect this relationship, we used the multiple mediation analysis (MMA) approach. The number of years of education mediated this relationship significantly in the right temporal lobe (indirect effect = 0.704, 95% CI (1.13, 0.001)) in the presence of potential mediators. These results provide evidence that life course factors are related to cortical ribbon complexity across adulthood and higher income and healthy lifestyle may be protective factors against age-related cognitive decline.

Acknowledgements: UK Biobank

Contact: n.nazlee.19@abdn.ac.uk

Abstract number: P20

Evaluation of the stiffness of flexor digitorum superficialis muscle using ultrasound shear wave elastography in healthy volunteer: a preliminary study

Phongpan Tantipoon[1], Markus Pakleppa[1], Zhihong Huang[1], Chunhui Li[1]

1. Biomedical Engineering, School of Science and Engineering, University of Dundee

Distribution of muscle stiffness plays an important role for human joint stability during the operation of functional movements. Ultrasound shear wave elastography (SWE) provides a reliable tool for quantifying tissue stiffness. However, applying this method to examine elastic properties of human muscles have been limited (Creze, et al., 2018). The purpose of this study focuses on evaluation of muscle stiffness using SWE to achieve better understanding of the function of human hand. In Addition, a method for the reliable stiffness evaluation of muscles with SWE are investigating. For preliminary work, muscle stiffness of a healthy volunteer is analysed. Flexor digitorum superficialis muscle is identified in B-mode ultrasound and then evaluated with SWE. Muscle stiffness is evaluated using a Verasonics research system (Vantage 128, Verasonics). Comb-Push ultrasound elastography (CUSE) approach is applied for data acquisition. Different intensity of muscle contraction is determined using digital hand dynamometer (CAMRY-EH101, China). The volunteer is instructed to grasp the dynamometer with 0%, 25%, 50%, 75% and 100% of the maximum voluntary contraction (MVC), respectively for acquiring the structural image of the muscle. Two-dimensional shear wave speed map is reconstructed. Velocity of shear wave propagation within the muscle is measured and muscle elasticity is calculated. The initial result revealed the tendency of the shear wave speed and muscle elasticity increase at higher intensity of muscle contraction. The mean (SD) of shear wave speed is ranged from 2.29(1.59) to 9.25(7.51) m/s for 0% and 100% MVC, respectively. Moreover, the mean of Young's modulus is ranged from 15.76 to 256.50 kPa for 0% and 100% MVC, respectively. The next steps of this study involve collecting data from a significant number of participants to determine the reliability of the method and comparison of muscle elasticity using SWE and digital palpation device, MyotonPro (Myoton AS, Estonia) or tactile imaging approach.

Contact: p.tantipoon@dundee.ac.uk

Abstract number: P21

Improving Needle Visualization in Ultrasound-Guided Regional Anaesthesia

Ashraf Agweder[1,2], Graeme McLeod[1], George Corner[1], Zhihong Huang[1]

1. School of Science and Engineering, University of Dundee, United Kingdom
2. Radiology Department, Faculty of Medical Technology, Benghazi, Libya

Introduction: Needle insertion has achieved popularity over the last few years, particularly in regional anaesthesia and towards achieving higher accuracy in terms of targeting and safety. Ultrasound guidance imaging is often applied within procedures. All the computational and experimental results indicate success and suggest that ultrasonic devices can give an accurate with regional anaesthesia. The outcomes are to: record real-time image, display the entire length of the needle on grayscale; assess the visibility of the needle close, on and in to the target; and measuring the force and pressure inside the tissue using ultrasound imaging technology to identify a moving needle tip.

Method: It has built a needle that can record the force and pressure in tissues via using sensors. A 20g needle block (150mm) was chosen for the insertion in a lamb leg and Gelatin phantom in three different points (upper, middle, lower). The needle was driven to the tissue by a motor stage at a velocity of 1.5 mm/s in three various angles (30, 45, and 60) degree. An ultrasound machine and linear transducer of 14-5 MHz applied to image the needle inside the tissues. It has measured the force continuously, whereas the pressure infused a 0.5ml pre/inside the nerve using Pendo Tech device pressure MAT device. In addition, a continuous Real-time needle location pressure applied via a Milestone (CompuFlo Instrument) that utilised to measure pressure changes through a different type of tissues.

Result: The results illustrate that the pressure and force reach a high point when the needle indenting to penetrates the tissue. Also, when the needle tip indenting gets in the nerve. The pressure was around 7-8 Psi in the Pendo Tech Pressure MAT device. While reaches around 200 mmHg in the milestone device when the needle indenting to hit the nerve and the force was around 0.3 mN at the same point.

Conclusion: The experiments carried out on a gelatin phantom and lamb leg tissue to determine force and pressure at the ultrasound of 14 MHz when the needle inside the tissue.

Contact: aafagweder@dundee.ac.uk

Abstract number: P22

Application of Swept-Source Optical Coherence Tomography (SS-OCT) System for Wound Healing Monitoring based on a Murine Model

Tianyu Zhang[1], Kanheng Zhou[1], Duo Zhang[1], Yubo Ji[1], Cash Jenna[2], Rocliffe Holly[2], Pellicoro Antonella[2], Zhihong Huang[1], Chunhui Li[1]

1. School of Science and Engineering, University of Dundee, Dundee, DD1 4HN
2. MRC Centre for Inflammation Research, The University of Edinburgh, The Queen's Medical Research Institute, Edinburgh, EH16 4TJ

It is crucial to understand the process underlying the wound healing process when investigating or evaluating therapeutic treatment to accelerate wound healing. The vascular change of the skin plays a vital role in different timeline of wound healing. Current traditional techniques (e.g., histology) are highly invasive, or lack the level of vascular detail required for evaluating the process of wound healing. Instead, optical coherence tomography (OCT) and OCT angiography (OCTA) is an ideal technique that can achieve real-time assessment of microstructure and microvascular in micron-level resolution.

Four full-thickness excisional wounds were made to the dorsal skin of the mice. A Swept-Source OCT (SS-OCT) system was used to examine the wound area of two mice in the process of wound healing Day3, Day7, Day10, Day 14 after injured and control data from adjacent healthy skin. Additionally, histology images are also acquired for the same timeline.

After the post-processing procedure based on the Elastix-registration algorithm and Eigen-Decomposition algorithm, en-face structural and vascular images were provided for spanning the whole wound healing process. Moreover, its corresponding cross-sectional structure images are generated and compared with its corresponding histology outcomes for a full understanding of the epidermal restoration and scar formation/loss during wound healing.

Furthermore, the SS-OCT system provides abundant information within different phases of wound healing demonstrates that our system provides a robust, qualitative, for serving as a standard model for further research into pharmacological and physical factors that are external to each other (e.g., laser light).

Contact: t.x.zhang@dundee.ac.uk

Abstract number: P23

Using deep learning and transfer learning to accurately assess the epithelial region in human skin based on Optical Coherence Tomography

Yubo Ji[1], Shufan Yang[2], Kanheng Zhou[1], Chunhui Li[1], Zhihong Huang[1]

1. School of Science and Engineering, University of Dundee
2. School of Computing, Edinburgh Napier University, Edinburgh, United Kingdom and Center of Medical and Industrial Ultrasonics, University of Glasgow, Glasgow, United Kingdom

Introduction: Identification and monitoring of the epidermis layer is important because thickness of the epidermis and the local shape of the dermal-epidermal junction (DEJ) are important factors in monitoring skin disease. Since optical coherence tomography (OCT) are real-time and non-invasive imaging techniques that can perform a cross-sectional evaluation of tissue microstructure, they are ideal systems to monitor the thickness of epidermal tissues in micron-level resolution. Traditional segmentation on epidermal regions was performed manually, which is time-consuming and impractical in real-time. In recent year, the automatic method like Deep convolutional neural networks (CNNs) have achieved great success in segmentation tasks due to their ability to learn high-level task-specific imaging features. In these approaches, accuracy and generalizability clinical data based on human are greatly limited. The use of mice models is an effective way of studying the layer information. We propose a transfer learning-based algorithm from CNN-based model in mice and it requires only a few batches training images of human skin data from OCT.

Method: We trained a CNN model based on 2000 expert-annotation B-scan images based on murine model. Then we applied transfer learning method to fine-tune the acquired model using a few batch (~50 images) expert annotation B-scan images based on human to. We evaluated the performance of this method 3 healthy skin site of 3 abnormal skin site in a clinical trial.

Result: Our method outperforms to other deep learning-based methods in matching expert manual segmentations using several evaluation metrics (F1_score, F2_score, Dice coefficient). The en-face epidermis thickness mapping and quantitative evaluation method is provided for different skin conditions (burning wound, inflammation and lipoma).

Conclusion: Our novel pipeline is able to provide the standardized and accuracy thickness measurement of epidermis from en-face reconstructed thickness mapping.

Contact: y.ji@dundee.ac.uk

Abstract number: P24

Viscoelastic properties of a corneal stromal model measured by surface acoustic wave optical coherence elastography (SAW-OCE)

Yilong Zhang, Kanheng Zhou, Chunhui Li, Zhihong Huang

School of Science and Engineering, University of Dundee, Dundee DD1 4HN, UK

Introduction: Collagen hydrogels seeded with keratocytes are popular for modelling the human corneal stroma in vitro. Viscoelastic properties including elastic modulus and viscosity are important parameters related to pathological conditions. However, the viscosity of corneal stromal model is lacking for quantitative studies. This study demonstrated a non-invasive approach to continuously monitor the cell-matrix viscoelastic properties in a reconstructed human corneal stromal model.

Methods: Hydrogel samples were manufactured with collagen concentrations of 3, 5 and 7 mg/mL. Keratocytes were seeded at 8 K per 80 uL hydrogel. Hydrogels without cells were controls. The hydrogels were examined every two days. The confluent of the keratocytes were monitored by a light microscope. The viscoelastic properties of the hydrogel were measured by a SAW-OCE system. The SAW pulse with maximum amplitude of 250 nm was induced on the sample surface by an air-pulse system. The air was delivered through a needle tip with a diameter of 0.15 mm. A customised phase sensitive (PhS)-OCT system with central wavelength of 1310 nm and sampling frequency of 20,730 Hz was applied to track the SAW pulse. The viscoelastic parameters were quantified by fitting the SAW phase velocity curve into a Rayleigh wave dispersion model. Moreover, a plate compression, ramp-hold relaxation test was used to validate the results from SAW-OCE. The maximum displacement of the hydrogels compressed by the plate was 1.5 mm (2 mm/min, 15% strain). Then, the hydrogels were held for 300 s to measure stress relaxation. Finally, the force-displacement data was fitted into Kelvin-Voigt fractional derivative (KVFD) model to obtain the viscoelastic parameters.

Results: Cell-seeded hydrogels with concentration of 3mg/mL had the greatest increase in cell proliferation. The correlation coefficient of the viscoelastic parameters obtained between plate compression relaxation test and air-pulse OCE were 98.67% and 92.25% for the viscosity and the elastic modulus, respectively. An increasing trend was observed in the viscoelastic properties for three collagen concentrations of the cell-seeded hydrogels and the lowest initial collagen concentration construct had the greatest increment. By contrast, the controls were stable over 11 days.

Contact: y.y.zhang@dundee.ac.uk

Abstract number: P25

Assessment of MR imaging quality with MRgFUS installation

McLellan K. [1], Summersgill J. [1], Gilbertson T. [2,3], Steele J.D. [3], Macfarlane J.A.[1,3]

1. Medical Physics Department, NHS Tayside
2. Neurology Department, NHS Tayside
3. University of Dundee

Introduction: University of Dundee has recently installed an Exablate Neuro (Insightec, Israel) MR-guided Focused Ultrasound to its 3T PrismaFIT (Siemens) to allow non-invasive transcranial neurosurgery. It is the second installation of its type in the UK, and the first in Scotland. The focused application of US beams to deep-brain substructures results in heating sufficient to cause ablation. Its use in patients with Essential Tremor has been approved by NICE1, replaces invasive procedures and is transformative. Its use in other neurological conditions is an area of active research.

During treatment, a 1024-element transducer is coupled to the patient's scalp using a frame and water bath. The physical size of the equipment precludes the use of standard head coils for imaging. Instead the integral body coil is used to receive signal.

Treatments involve 'rest' periods during which US is not applied. Our aim was to assess the image quality we might achieve if we used that time to acquire intra-treatment neuroimaging data.

Methods: QA measurements were acquired before and after installation, including uniformity, SNR, geometric distortion.

A healthy volunteer underwent a standard neuroimaging procedure T1-MPRAGE, T2, SPACE and finger-tapping fMRI using the 20-channel head and neck coil, repeated using the body coil, in the absence of the Exablate head-frame or water bath.

Results: No qualitative deterioration in QA image quality was observed.

Significant reduction in image quality was seen when using the body coil to receive data. Despite significant reduction in SNR, BOLD activations were demonstrated in the motor cortex.

Discussion: Acquisition of data using the body rather than head coil results in a significant degradation of image quality. Surprisingly, motor BOLD responses were still detectable.

It is anticipated that the presence of head frame, water bath and transducer array will have further impact on field homogeneity and image quality.

References:

1. NICE Guidelines: Unilateral MRI-guided focused ultrasound thalamotomy for treatment-resistant essential tremor. Interventional procedures guidance [IPG617] 20 June 2018

Contact: katherine.mclellan@nhs.scot

Abstract number: P26

Is diagnostic imaging of the breast possible with a Magseed in situ?

Jennifer A Summersgill[1], Jennifer A Macfarlane[1], Yee Ting Sim[1], Andrew Evans[1], Sandra Gawley[1], Mark Worrall[1]

1. Clinical Research and Imaging Facility, University of Dundee

Purpose: To quantify the CT and MRI susceptibility artefact of a 5mm MAGSEED breast marker constructed of surgical grade stainless steel. This will determine whether a patient with this marker in situ can undergo diagnostic breast imaging.

Methods: Phantom testing was done on MRI and CT. Additionally a healthy volunteer was scanned using MRI with the marker on the skin surface. All MRI was performed at 3T using our clinical breast protocol which included spin echo, gradient echo, DWI and dynamic sequences. CT scanning was performed with filtered back projection and iterative reconstruction to compare techniques.

Results: On MRI spin-echo sequences the artefact diameter was 4.1cm in-vivo, consistent with the manufacturer guidance. For gradient echo and DWI the artefact ranged from 4.7 cm to 5.8 cm. Fat saturation was unsuccessful with the marker in dynamic imaging resulting in a much larger artefact of 9.5 cm. 3D surface rendering of the in-vivo MRI showed a butterfly distribution of the artefact. On CT the artefact was limited to the size of the marker and remained unaffected by reconstruction technique.

Conclusion: Non-breast MRI with the marker in situ can be performed safely while retaining diagnostic quality of images. The presence of the marker in breast MRI causes significant artefact up to 9.5cm from the marker rendering anatomy within this region non-diagnostic. Patients with this marker in situ are unlikely to benefit from an MRI breast exam until after the marker has been removed. CT imaging is unaffected by the presence of the marker.

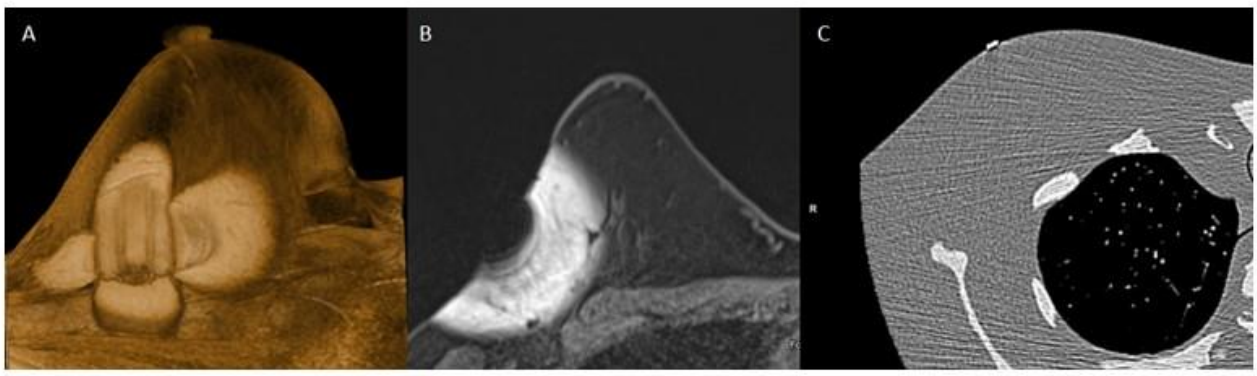

Figure 1: Three images from different scanning performed with the Magseed. A – 3D surface render of Magseed artefact on MRI imaging of a healthy volunteer on a T1 dynamic gradient echo sequence. B – Magseed artefact with area of failed fat saturation on a T1 dynamic gradient echo sequence. C – CT artefact measuring 5mm of Magseed positioned R>>L.

Contact: jennifer.summersgill@nhs.scot

Abstract number: P27

Optimising Navigator Scans for Use in MRI Prospective Motion Correction

Steven Winata[1], Daniel Hoinkiss[2], Graeme Keith[1], David Porter[1], Matthias Günther[2]

1. Imaging Centre of Excellence, University of Glasgow
2. Fraunhofer Institute of Digital Medicine MEVIS, Bremen, Germany

Introduction: Longer scan times in MRI make it prone to motion artifacts. Hardware and software-based techniques to reduce these effects have been proposed [1]. An example is Multislice Prospective Acquisition Correction (MS-PACE)[2]. The technique works by acquiring navigator slices to detect object motion, registering them to a reference volume and then prospectively correcting the scan orientation[2]. In this study, we investigated the effects of employing variable numbers of navigator slices on the technique's performance in detecting motion.

Methods: The study was performed using retrospective reconstruction of gradient-echo echo planar imaging time series (98 volumes, 39 slices, TR/TE 3000/30ms) acquired from a subject on a Siemens MAGNETOM Skyra 3T scanner. The motion protocol was: 1) facing down; 2) facing up; 3) back to start and 4) right tilt. The motion parameters were calculated using an algorithm developed in Siemens' Image Calculation Environment. The use of 2-18 equidistantly-spaced navigator slices was simulated and compared to a full-volume registration [3].

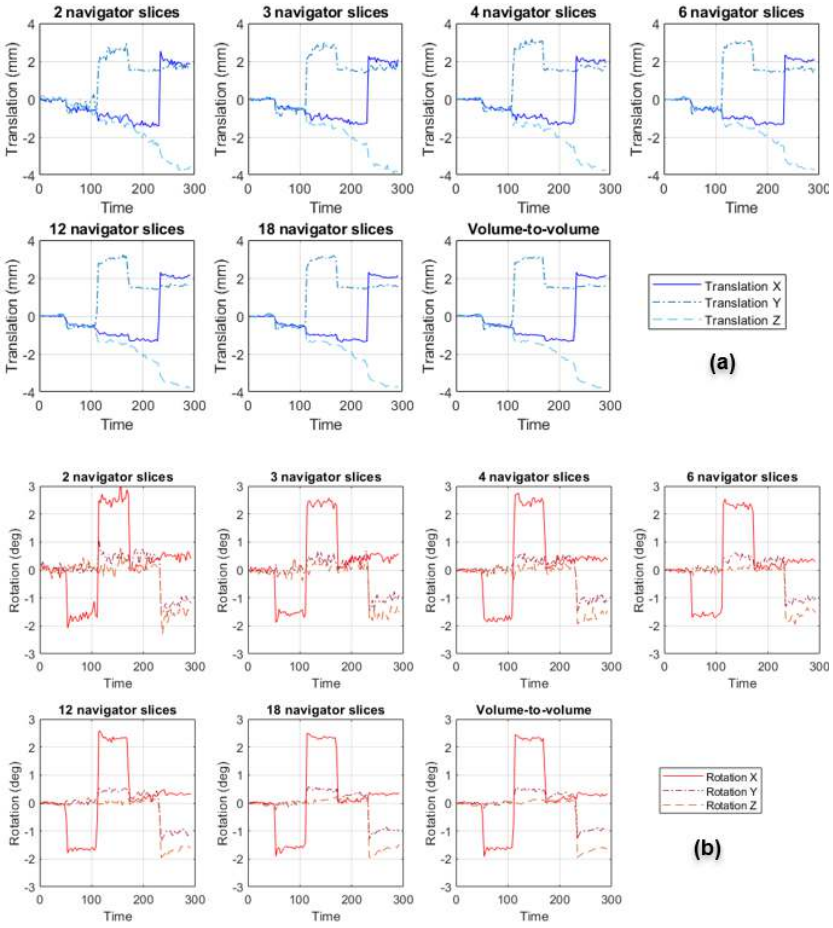

Fig 1. Translational (a) and rotational (b) parameters of the different scenarios.

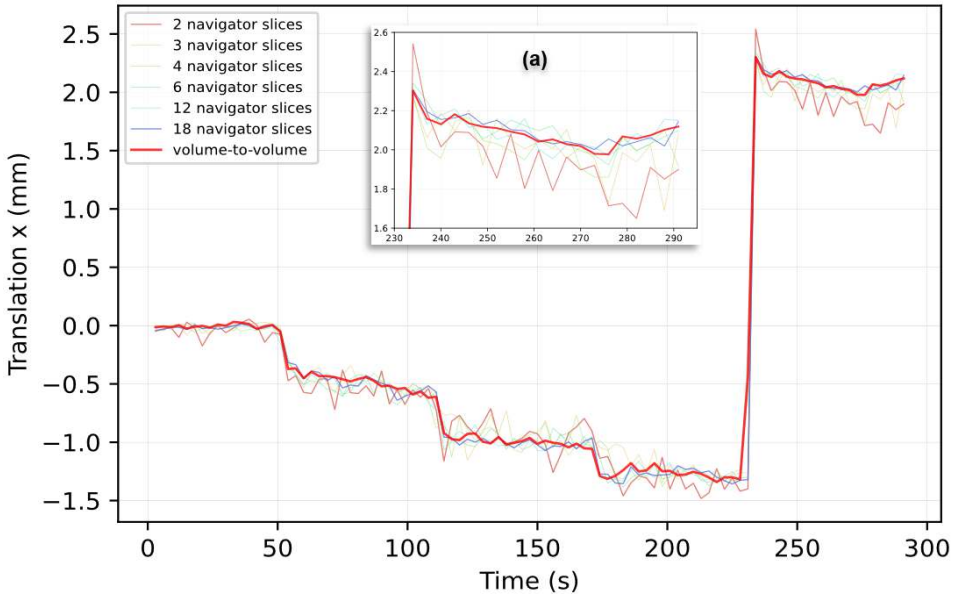

Fig 2. X-axis translational parameters. The red curve signifies the reference full-volume registration. The fewest (2) and the most (18) navigator slices cases are highlighted with bolder colours. The inset (a) focuses on the 230-300s time window. The jump at 230s is caused by the right tilting motion.

Discussion: Fig 1 shows the use of fewer navigator slices can achieve a registration accuracy comparable to full-volume registration. Further in vivo studies are planned for validation and evaluation of other effects of using fewer slices. Overall, these results suggest that the usage of as few as two navigator slices is feasible.

References:

1. Zaitsev et al. JMRI. 2015;49:887-901.

2. Hoinkiss DC, Porter DA. Magn Reson Med. 2017;78(6):2127-35.

3. Thesen S et al. Magn Reson Med. 2000;44(3):457-65.

Acknowledgements: The authors would like to thank the SINAPSE's Postdoctoral and Early Career Researcher Exchange programme for funding this project.

Contact: s.winata.1@research.gla.ac.uk

Abstract number: P29

RF simulations of cranial fixation plates in 7 tesla MRI

Andrew McDevitt[1], Sarah Allwood-Spiers[2], Shajan Gunamony[1], Paul McElhinney[1]

1. Imaging Centre of Excellence, University of Glasgow, Glasgow
2. Department of Clinical Physics and Bioengineering, NHS Greater Glasgow and Clyde

MRI is a non-ionising method of obtaining anatomical information which has been extensively used since the 1980s. Recent developments including the implementation of a 7T MRI scanner based at the Imaging Centre of Excellence, Glasgow offers a host of improvements. Neuroimaging at 7T has the potential to be a more powerful diagnostic tool due to an improved SNR, developed spectral resolution, and enhanced image quality. However, safety information is under-represented at this stronger field, for example, testing of passive medical implants, many of which are yet to be verified for safety at 7T.

A study run by Kraff et al [1] was conducted to assess heating of cranial fixation plates at 7T; they noted that using (12.5x12.5mm2) cranial fixation plates yielded no significant heating post craniotomy using their coil model. However, for other coils, a 10% reduction in power was recommended to account for variation in Specific Absorption Rate (SAR) until the simulations specify otherwise.

This paper aims to use simulations to establish how the presence of cranial fixation plates affects SAR distribution in the head for 7T scanning using a computer model of our 8-channel head coil, which was designed and built at the University of Glasgow and is now in use in a clinical setting. The software CST Studio Suite [Dassault Systems, France] allows us to accurately estimate the SAR in voxel models such as Duke which mimics a grown man. Initial simulations involved modelling two overlapping coils as shown in figure 1. Figure 2 shows the cranial fixation plates placed into the skull of Duke. We investigated how both E-field and SAR vary dependent on location of these plates including spacing of the plates from one another. From here, the full coil model for the 8-channel transmit coil was introduced to view how the SAR distribution changes.

Contact: 2587122m@student.gla.ac.uk

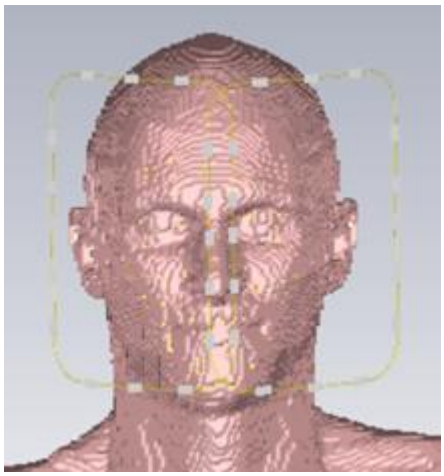

Figure 1

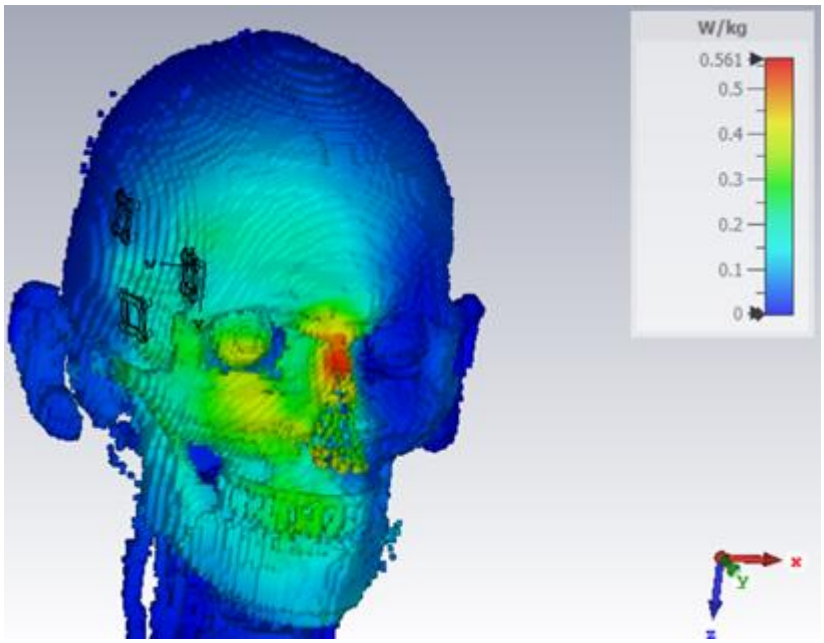

Figure 2

Abstract number: P30

Ex-vivo investigation of inflammation and thrombus PET radiotracers in lung, heart and brain tissue from COVID-19 related deaths

Matthew Pugh[1], Timaeus E. F. Morgan[2,3], David E. Newby[2], Norman Koglin[4], Sally L. Pimlott[5,6], Christophe Lucatelli[3], Andrew Sutherland[7], Paul G. Murray[8], Graham Taylor[1], Adriana A.S. Tavares[2,3], **Mark G. MacAskill**[2,3]

1. Institute of Immunology and Immunotherapy, University of Birmingham, Birmingham, UK
2. University/BHF Centre for Cardiovascular Science, University of Edinburgh, Edinburgh, UK
3. Edinburgh Imaging, University of Edinburgh, Edinburgh, UK
4. Life Molecular Imaging, Germany
5. School of Medicine, University of Glasgow, Glasgow, UK
6. NHS Greater Glasgow and Clyde, Glasgow, UK
7. WestCHEM, School of Chemistry, University of Glasgow, Glasgow, UK
8. Health Research Institute, University of Limerick, Limerick, Ireland

Introduction: COVID-19 infection is associated with a systemic inflammatory response and emerging data suggests that this has an impact beyond the lungs. In addition, there have been widespread reports of thrombosis in patients with COVID-19. We investigated inflammation with TSPO expression (mainly associated with the innate immune response) and the thrombosis with glycoprotein IIb/IIIa expression (present on activated platelets) in lung, heart and brain tissue from COVID-19 related deaths and matched non-COVID-19 controls. We hypothesised that increased systemic inflammation and thrombosis would be associated with COVID-19.

Methods: Ethical approval was obtained from the Newcastle North Tyneside 1 research ethics committee (IRAS 197397). Formalin fixed paraffin embedded and sectioned lung, heart and brain tissue was used from 8 individuals who died from COVID-19 related causes (5 females, 3 males, mean age 74±11 years) and 8 individuals who died from non-COVID-19 related causes (5 females, 3 males, mean age 69±12 years). Autoradiography was performed using [18F]LW223 (TSPO) and [18F]GP1 (glycoprotein IIb/IIIa) using 1nM of radiotracer, with a non-specific binding control (10 µM). [18F]LW223 was quantified as the target to non-target (T:NT) relative to the unblocked signal. [18F]GP1 was qualitatively assess as present or not present.

Results: [18F]LW223 binding was detected throughout the lung, heart and brain. There were no differences in [18F]LW223 T:NT between the COVID-19 and control groups for either organ. In contrast, [18F]GP1 binding was lower and only sporadically present; lung control (5 out of 8) and COVID-19 (3 out of 8), heart control (0 out of 8) and COVID-19 (1 out of 8), brain control (1 out of 7) and COVID-19 (2 out of 4).

Conclusion: While this study is small, it clearly indicates that there are no marked changes in TSPO or glycoprotein IIb/IIIa expression in individuals who have died from COVID-19 related causes.

Contact: mark.macaskill@ed.ac.uk

Abstract number: P31

Characterisation of a Diffusion Phantom used for Diffusion MRI QA

Christopher Taylor[1], Dr Stephen Gandy[1]

1. Medical Physics Department, Ninewells Hospital Dundee

Background: Diffusion weighted imaging (DWI) is routinely used in MRI examinations at NHS Tayside to aid in the diagnosis, staging and evaluation of the response to therapy for cancer patients. DWI provides a quantitative measure of water motion with the patient's tissue. The apparent diffusion coefficient (ADC) value can indicate whether a region or lesion is likely to be malignant or benign, and this can influence patient outcomes. It is therefore important that the reported ADC value is consistent and reproducible. NHS Tayside has purchase the HQ imaging DWI Phantom, with the aim of producing a quality assurance (QA) program for DWI. The initial step for this project has been to characterise the phantom T1, T2 and ADC values.

Methods: The phantom is comprised of two main compartments, A and B. It has a resolution test object and 6 'lesions', ranging in diameter from 2-10 mm. The T1 was measured in the uniform regions of both compartments A and B by modelling the saturation recovery and inversion recovery curves. The T2 values for the uniform regions within each compartment were obtained using a single slice multi-echo spin echo sequence with varying echo times. The ADC value was obtained using a Siemens clinical prostate MRI sequence, with b-values of 50, 400, and 800 s/mm2.

Results: The T1 values were successfully obtained using Saturation recovery and Inversion recovery for both compartments of the phantom. The T2 was also recorded for both compartments. The ADC values were recorded for all 6 lesions, and also for the uniform region of each compartment.

Conclusions: The phantom has successfully been characterised at 3T. This has provided useful information that will guide the use of the phantom for DWI QA and sequence optimisation.

Contact: christopher.taylor2@nhs.scot

Abstract number: P32

Lymph node characterisation of a metastatic mouse model of CRC using pre-clinical ultrasound

Marion Bacou[1], Vidya Rajasekaran-Sutherland[1], Katarzyna Kaczmarek[2], Adrian Thomson[1], Susan Moug[3], Helen Mulvana[2], Carmel Moran[1], Susan Farrington[1]

1. Edinburgh Cancer Research Centre, University of Edinburgh
2. Biomedical Engineering University of Strathclyde
3. NHS Greater Glasgow and Clyde

Lymph node metastasis is an important factor to consider for prognosis and therapy planning for numerous cancers including colorectal and anal cancer.

Whilst MRI and CT imaging, routinely used for cancer diagnosis, are highly efficient at detecting primary tumours, these techniques remain limited for the characterisation of sentinel lymph nodes. Recently, modern ultrasound scanners have improved precision imaging and widened applicability, providing high spatial and temporal resolution, 3D images, colour flow and power Doppler collection.

In this study, we developed a pre-clinical lymph node metastasis model by using intestinal organoids generated from intestinal tumours of KPN (villinCreER/KrasG12D/+/Trp53fl/fl/Rosa26N1icd) mouse model. Hock injections of KPN tumour organoids resulted in primary tumour formation in the hind leg and lymph node metastases in the leg-draining lymph nodes from 4 weeks post injection. The aforementioned lymph nodes were imaged with VEVO3100 preclinical ultrasound scanner at several timepoints before and after visual detection of the leg tumour to assess their volume, morphology and flow dynamics (3D ultrasound imaging and CEUS). Pathological examinations were also carried out on the excised lymph nodes after animals reached an end-point and compared to the obtained ultrasound images. The ultrasound images indicated abnormal lymph node enlargement before visual detection of a leg tumour, showing potential for improving pre-clinical diagnosis.

Acknowledgements: This work was funded by CRUK (A23333)

Contact: m.bacou@sms.ed.ac.uk

Abstract number: P34

SAR Simulation of a Close-fitting 8-channel Transceiver Head Coil Including EEG Electrodes for Safety Validation at 7T

McElhinney, P.[1], Paterson, G. [1], Philiastides, M.[1] and Gunamony, S.[1]

1. Imaging Centre of Excellence, University of Glasgow, Glasgow

Simultaneous use of EEG and fMRI in the study of dynamic brain function can offer greater insight than either method achieves in isolation. With the greater spatial resolution at ultra-high field MRI (UHF, ≥7T) the development of a simultaneous EEG-fMRI at 7T proves a fertile field for investigation [1-4]. A close-fitting oblate rectangular profile was conceived and simulated using CST Microwave Studio with 8 overlapping rectangular loops to provide inductive decoupling between channels. Tuning and optimization was carried out in simulations using our head phantom, both with and without the addition of the EEG electrodes [5, 6]. Once the final model was optimized, a further set of human body models were simulated with and without the EEG electrodes once again. The model including the EEG electrodes has 66 PEC loops. The EEG electrodes are connected to a common port via CST 'bond wires,' which have the characteristics of a perfect conductor. Each of these contains a 10KΩ resistor (not shown) and the location of the port is approximately 5 cm above the location of the electrode CPz.

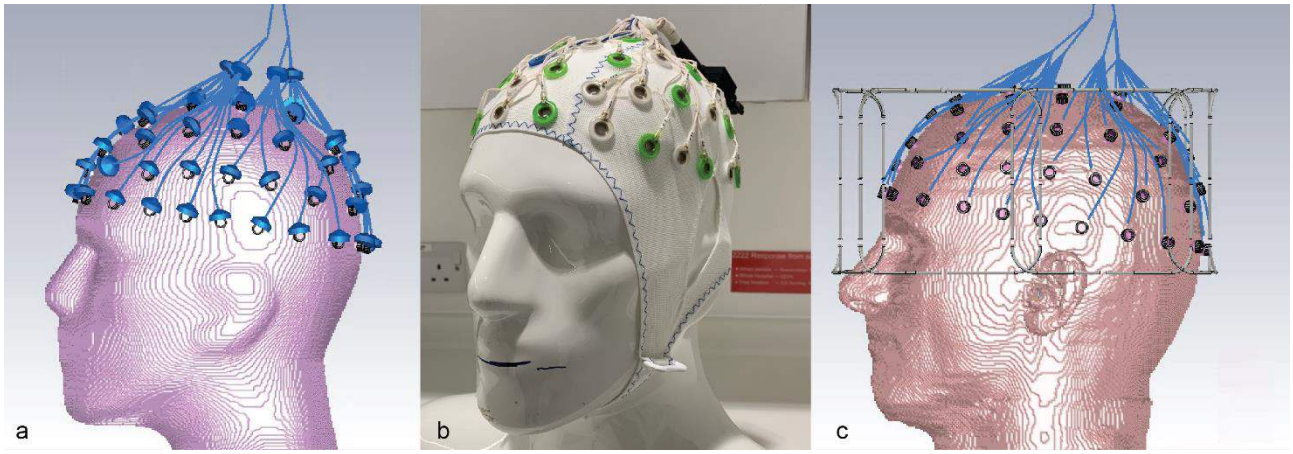

Figure 1

The maximum SAR value was calculated as 0.52 W/kg for a 1W signal in the Duke model 15mm into the coil. The inclusion of the EEG cap altered the location of the maximum SAR in the Duke model, where it is now located at the posterior, in a position close to the overlap between coils and electrodes. While these results demonstrate that the EEG cap does influence the distribution of the SAR, we do not see any significant increase in the overall magnitude and they provide a strong basis for the overall safety and fundamental design of this coil and EEG system. Allowing development of this prototype to continue through towards subject trials in the near future.

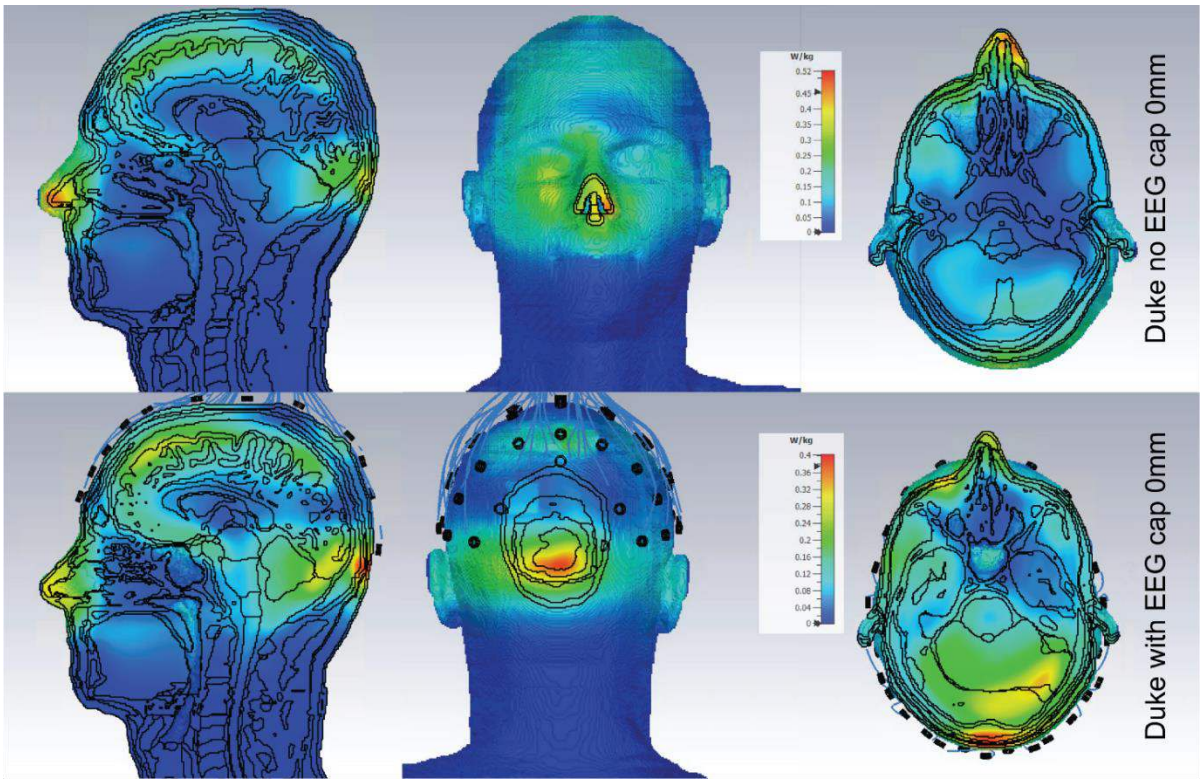

Figure 2

1. Pisauro M, Fouragnan E, Retzler C et al. Neural correlates of evidence accumulation during value-based decisions revealed via simultaneous EEG-fMRI. Nat Commun 8, 15808 (2017)

2. Fouragnan, E., Retzler, C., Mullinger, K. et al. Two spatiotemporally distinct value systems shape reward-based learning in the human brain. Nat Commun 6, 8107 (2015)

3. F. Pittau et al., 'Simultaneous Eeg and Functional Mri at Ultra-High Field (7t) in Epilepsy: Feasibility and First Results', Epilepsia, vol. 57, pp. 24–25, Dec. 2016.

4. J. Jorge, F. Grouiller, R. Gruetter, W. van der Zwaag, and P. Figueiredo, 'Towards high-quality simultaneous EEG-fMRI at 7 T: Detection and reduction of EEG artifacts due to head motion', Neuroimage, vol. 120, pp. 143–153, Oct. 2015

5. M. C. Meyer, R. Scheeringa, A. G. Webb, N. Petridou, O. Kraff, and D. G. Norris, 'Adapted cabling of an EEG cap improves simultaneous measurement of EEG and fMRI at 7T', J. Neurosci. Methods, vol. 331, p. 108518, Feb. 2020, doi: 10.1016/j.jneumeth.2019.108518.

6. Jorge J, Grouiller F, Ipek O et al. Simultaneous EEG–fMRI at ultra-high field: Artifact prevention and safety assessment. Neuroimage 105 (2015) 132-144.

Contact: paul.mcelhinney@glasgow.ac.uk

Abstract number: P35

Contrast enhanced magneto-motive ultrasound (CE- MMUS) as a promising imaging technique for improved lymph node identification

Katarzyna Kaczmarek[1], Sandra Sjöstrand[2], Adrian Thomson[3], Tomas Jansen[2], Carmel M. Moran[3], Helen Mulvana[1]

1. Department of Biomedical Engineering, University of Strathclyde, Glasgow, UK
2. Department of Biomedical Engineering, Lund University, Lund, Sweden
3. Centre for Cardiovascular Science, University of Edinburgh, Edinburgh, UK

Identifying cancerous lymph nodes in the early stage of colorectal cancer is a crucial factor for optimal disease staging. One of the methods able to identify sentinel lymph nodes (SLN) is an ultrasound imaging technique called magneto-motive ultrasound (MMUS). In the MMUS, SPIONs (superparamagnetic iron-oxide nanoparticles) drain to the SLN through the lymphatic drainage move, and the applied alternating magnetic field creates a tissue-laden movement that can be imaged with ultrasound. Based on a subsequent post-processing it is possible to filter out the known MMUS frequency (doubled oscillation frequency) and recover the ultrasound imaged displacement of lymph nodes containing SPIONs.

Our study proposes a novel approach that has a potential to improve the MMUS sensitivity using microbubbles with SPIONs attached (SPION-MBs). We expect SPION-MBs will generate larger tissue displacement and therefore enable easier distinction between tissues containing SPION-MBs from their surroundings, where COMSOL simulation supports our hypothesis [1, 2].

Prior to assessing SPION-MBs, we first seek to establish MMUS parameter space that would define what SPION concentration, stiffness of tissue-mimicking material (TMM), strength and frequency of magnetic field will be most beneficial for the detection of the MMUS displacement. The experimental MMUS setup consists of the TMMs (PVA, agar), VisualSonics 3100 and custom made magnetic coil. Subsequent, post-processing and data analysis to filter out the nanoparticle-induced movements and uncover MMUS displacement is conducted with the MATLAB software.

We expect to demonstrate MMUS ability to detect stiffness, accuracy in detecting small size inclusions and present improved MMUS sensitivity after SPION-MBs incorporation. We believe that CE-MMUS shows promise as an imaging approach to improve sentinel lymph nodes identification and outperform other imaging techniques as it is cost-effective, portable and non-ionizing.

1. Sjöstrand S. et al., IEEE International Ultrasonics Symposium (IUS), 2019

2. Evertsson M. et al., IEEE International Ultrasonics Symposium (IUS), 2015

Acknowledgements: The work was supported by Cancer Research UK [A23333].

Contact: katarzyna.kaczmarek@strath.ac.uk